AD_____

Award Number:
W81XWH-06-1-0429

TITLE:
Role of X-linked Inhibitor of Apoptosis in Breast Cancer

PRINCIPAL INVESTIGATOR:
Karolyn Oetjen, B.S.

CONTRACTING ORGANIZATION:
Regents of the University of Michigan
Ann Arbor, MI 48109-1274

REPORT DATE:
April 2009

TYPE OF REPORT:
Final Report

PREPARED FOR: U.S. Army Medical Research and Materiel Command
Fort Detrick, Maryland 21702-5012

DISTRIBUTION STATEMENT:

X Approved for public release; distribution unlimited

REPORT DOCUMENTATION PAGE

Form Approved
OMB No. 0704-0188

1. REPORT DATE *(DD-MM-YYYY)*	**2. REPORT TYPE**	**3. DATES COVERED** *(From - To)*
01-04-2009	Final Report	15 March 2006-14 March 2009

4. TITLE AND SUBTITLE

Role of X-linked Inhibitor of Apoptosis in Breast Cancer

5a. CONTRACT NUMBER

5b. GRANT NUMBER
W81XWH-06-1-0429

5c. PROGRAM ELEMENT NUMBER

6. AUTHOR(S)

Karolyn Oetjen

5d. PROJECT NUMBER

5e. TASK NUMBER

5f. WORK UNIT NUMBER

7. PERFORMING ORGANIZATION NAME(S) AND ADDRESS(ES)

Regents of the University of Michigan
Ann Arbor, MI 48109

8. PERFORMING ORGANIZATION REPORT NUMBER

9. SPONSORING / MONITORING AGENCY NAME(S) AND ADDRESS(ES)

U.S. Army Medical Research and Materiel Command
Fort Detrick, Maryland 21702-5012

10. SPONSOR/MONITOR'S ACRONYM(S)

11. SPONSOR/MONITOR'S REPORT NUMBER(S)

12. DISTRIBUTION / AVAILABILITY STATEMENT

Approved for public release; distribution unlimited

13. SUPPLEMENTARY NOTES

14. ABSTRACT

XIAP has been identified as a potential target for breast cancer therapeutics, but the specific functions of XIAP that contribute to breast cancer development or progression remain unknown. The major tasks for this phase of this project involved evaluating breast cancer cell lines depleted in XIAP expression in tumor growth models in vivo and anchorage-independent growth models in vitro. Surprisingly, XIAP did not affect cancer cell growth in these models, and cell lines with rescued expression of XIAP did not demonstrate increased tumorigenesis compared to XIAP-deficient cells. These cell lines have been evaluated for sensitivity to apoptotic stimuli, and XIAP was a necessary anti-apoptotic molecule in these cells and required caspase-inhibitory residues D148 and W310 for this activity. This knowledge will be valuable to guide the development of therapeutics that target XIAP, which are currently in phase I/II clinical trials.

15. SUBJECT TERMS
Apoptosis, Breast Cancer, X-linked Inhibitor of Apoptosis

16. SECURITY CLASSIFICATION OF:			**17. LIMITATION OF ABSTRACT**	**18. NUMBER OF PAGES**	**19a. NAME OF RESPONSIBLE PERSON**
					USAMRMC
a. REPORT	**b. ABSTRACT**	**c. THIS PAGE**	UU	32	**19b. TELEPHONE NUMBER** *(include area code)*
U	U	U			

Standard Form 298 (Rev. 8-98)
Prescribed by ANSI Std. Z39.18

Table of Contents

Introduction

Pre-clinical evidence suggests that X-linked Inhibitor of Apoptosis (XIAP) is an exciting potential target for breast cancer therapeutics, which provides strong motivation for the role of XIAP in breast cancer to be fully elucidated. XIAP is involved in multiple cellular functions that have been implicated in breast cancer. This project seeks to identify the properties of XIAP that play a crucial role in breast cancer, by examining mutated XIAP molecules that are deficient in specific cellular functions in both *in vitro* and *in vivo* models of breast cancer.

Body

A number of pre-clinical studies have indicated that XIAP is a promising therapeutic target to sensitize malignant cells to chemotherapeutic agents in breast cancer and a number of other cancers. In order to establish models in which to evaluate the role of XIAP in breast cancer development, breast cancer cell lines were evaluated to identify appropriate cells for *in vivo* and *in vitro* models of breast cancer cell growth. In our experiments, I decided to utilize MDA-MB-231 cell lines obtained from Marc Lippman. These cells generate xenograft tumor growth in mice and anchorage-independent growth *in vitro*. Specifically, in soft agar culture suspended MDA-MB-231 cells grow into colonies over four to six weeks. In athymic nude mice, subcutaneous injection of MDA-MB-231 cells results in tumor development within four to six weeks. The tumor mass primarily consists of cells with advanced grade adenocarcinoma morphology and areas of necrosis on histologic examination. In establishing these models, I completed task 1 of the project.

To examine the effect of XIAP using the models of breast cancer established, I developed cell lines deficient in XIAP expression. The development of these cells was described in a previous report and is briefly described here. Short hairpin RNA sequences (shRNA) were utilized to suppress XIAP expression using RNA interference (RNAi). These shRNA sequences were introduced into the cell lines using lentiviral vectors, resulting in integration into the genome and stable suppression of XIAP (Fig. 1A). Stable, rather than transient, disruption of XIAP is necessary for the long duration of the *in vivo* and *in vitro* experiments proposed. The lentiviral vectors contain fluorescent markers, and cells were confirmed to express fluorescent proteins by FACS or by fluorescence microscopy (Fig. 1B) and to demonstrate suppression of XIAP protein by Western blot (Fig. 1C). For these experiments, I used two different XIAP shRNA sequences, in addition to cell lines with two different control shRNA sequences. These independently targeted cell lines will be particularly valuable for identifying non-specific effects that could result from RNAi, lentivirus infection or off-target effects of an shRNA sequence. The focus of this project is to study specific mutations in XIAP that disrupt its caspase-dependent and -independent functions (Lewis, 2004). Re-introduction of XIAP is accomplished by stable expression of RNAi-resistant lentiviral

vectors, which allows the expression of mutated XIAP proteins to replace endogenous XIAP (Fig. 2A). I expressed wild-type XIAP, XIAP D148A, XIAP W310A or the double mutant XIAP D148A W310A in the cells previously suppressed in XIAP expression. As before, XIAP expression was confirmed by Western blot (Fig. 2B). Establishment of these lentiviral constructs and cell lines completed task 2 of the project.

In task 3, I characterized the growth of XIAP-deficient breast cancer cell lines *in vitro.* Using the soft agar growth assay established in task 1, I examined foci formation of XIAP-deficient breast cancer cell lines. XIAP-deficient cells did not demonstrate a difference in the number of foci formed following growth in soft agar (Fig. 3A). I also confirmed the growth rates of XIAP-deficient cell lines under normal culture conditions in tissue culture plates with 10% fetal bovine serum, and did not observe a change in proliferation under normal cell culture conditions (Fig. 3B).

I have extensively examined the contributions of XIAP during growth of breast cancer cells *in vivo* using the xenograft tumor model establish as part of task 1. We first examined the growth of XIAP-deficient cells during tumor formation following subcutaneous injection in immunodeficient mice. Using rigorous techniques minimized variance in tumor size. XIAP-deficient and control cells were harvested from culture at identical cell density to ensure similar growth kinetics. XIAP-deficient and control cells were injected on opposite flanks of the same mouse, in order to minimize the effects of mouse-to-mouse variation. Furthermore, mice were anesthetized during injection to ensure complete subcutaneous delivery of cells. The results of these experiments, shown in Figure 4, indicate that loss of XIAP correlates with a trend of delayed tumor growth in athymic nude mice. XIAP-deficient MDA-MB-231 cells were capable of forming large tumors at some injection sites, but at many injection sites growth was delayed 1-2 weeks. However, statistical analysis of tumor growth using a paired two-way ANOVA did not reveal statistically significant changes in tumor size compared to control shRNA tumor growth. We confirmed that expression of XIAP was suppressed in tumors at sites injected with XIAP-deficient cells. At the study endpoints, tumors were harvested and analyzed by Western blot for XIAP expression, shown in Figure 5A. Moreover, tumors from mice injected with XIAP-deficient and control cells were also sub-cultured *ex vitro*. Cells cultured from the tumor explants express appropriate fluorescent markers, indicating that they originated from the injected cells (Fig 5B). In the case of cells from XIAP shRNA expressing tumors, XIAP expression continues to be greatly diminished on Western blot in cultures of tumor cells *ex vivo* (Fig. 5C). These results confirm that tumors observed following injection of XIAP-deficient cells were not the result of proliferation of a subpopulation of cells with intact XIAP expression.

We further examined the trend of decreased tumor growth in XIAP-deficient cells by generating additional cell lines expressing XIAP shRNA, using a distinct but similar sub-clone of MDA-MB-231 cells. In tumors that developed from these cells, shown in Figure 6A, differences between XIAP-deficient and control cells were small and were not statistically significant using paired two-way ANOVA. At the study endpoint, tumors mass was measured, shown in Figure 6B, and tumor size was unaffected by suppression of XIAP. Based on these findings, we returned to the previous set of XIAP-deficient cell lines

(Fig 4), in order to evaluate whether these cells would be a feasible model for examination of the effect of XIAP mutations on tumor development. We injected XIAP-deficient cancer cells expressing either vector or RNAi-resistant XIAP and monitored subcutaneous tumor growth, shown in Figure 7. Re-expression of XIAP was unable to rescue tumor growth, suggesting that the changes in tumor development observed in Figure 4 are non-specific – not the direct effect of XIAP. While some previously published results demonstrate a critical role for XIAP in tumor growth (LaCasse 2006, McManus 2004), another study confirms the findings reported here, that XIAP is not required for tumor growth (Ravi 2006). Although we attempted to use a long-term, non-pharmacological approach to investigate the effects of XIAP on breast cancer development, these conflicting results have led us to re-evaluate this model. Indeed, a very recent publication has questioned the relevance of xenograft models using cultured cell lines, in particular for the effects of in vitro cell culture on expression of pro- and anti-apoptotic proteins (Daniels 2009). The results reported in my studies have informed other investigations in our laboratory, which led to the development of an autochonous model of tumor growth to examine the role of XIAP. Our laboratory researched the effect of XIAP using a genetically targeted mouse that develops prostate tumors, which led to the discovery that XIAP is not required for prostate cancer development or progression (Hwang 2008). Thus, the contributions of XIAP to tumor development are more subtle than previously thought. XIAP might in fact remain a valuable target in breast cancer therapeutics, but our studies have demonstrated that stable suppression of XIAP is not a feasible model of the potential effects of acute interference with XIAP during pharmacologic treatment. The potential for XIAP as a viable target for cancer therapeutics continues to be advanced, with promising results in phase I clinical trials (Dean 2009).

In task 5, I aimed to establish whether loss of XIAP in these cancer cell lines affects apoptosis. During initial experiments, I found that there is no difference in viability between XIAP-deficient cells and controls following treatment with apoptotic stimuli for up to 24 hours (Fig. 8A). However, in further experiments the effect of XIAP on cell death can be seen at later times, 48 to 72 hours following apoptotic stimuli (Fig. 8B). These results confirm that the XIAP-deficient cell lines used in the tumor studies are more sensitive to apoptotic stimuli, and related studies have been published by our laboratory for cancer cell lines derived from colon carcinoma (Galban 2009). In all, these studies confirm that XIAP does play a role in apoptosis in breast cancer cell lines, which was dependent on the caspase inhibitory activity (D148 W310) and ubiquitin ligase activity (H467) of XIAP, as demonstrated with mutant XIAP expression in breast cancer cells lines in Figure 9.

Key Research Accomplishments

- XIAP expression can be effectively suppressed using lentiviral introduction of shRNA in breast carcinoma cell lines.

- Suppression of XIAP persists in tumors *in vivo* and tumor explants *ex vivo*.

- Loss of XIAP does not alter breast cancer cell growth under normal culture conditions *in vitro* or in xenograft tumor growth *in vivo*.

- Loss of XIAP increases sensitivity to apoptotic stimuli, which is dependent on D148 and W310 residues.

Reportable Outcomes

Bibliography of publications and meeting abstracts for the principal investigator. No other personnel received funding from this award.

- Presenting author: University of Michigan Medical Scientist Training Program Retreat, Roscommon, MI, Aug 3-5, 2007 (abstract and poster). “The Role of X-linked Inhibitor of Apoptosis in Cancer Development and Progression,” Karolyn Oetjen, Clara Hwang, David Kosoff, Kirk Wojno and Colin Duckett.

- Presenting author: University of Michigan Medical Scientist Training Program Retreat, Roscommon, MI, Aug 2006 (abstract and poster). “Role of X-linked Inhibitor of Apoptosis in prostate cancer development,” Karolyn Oetjen, Clara Hwang, David Kosoff and Colin Duckett.

- Presenting author: University of Michigan Medical Scientist Training Program Retreat, Roscommon, MI, Aug 2008 (abstract and poster). “Innate immune responses to lipopolysaccharide require c-IAP1,” Karolyn Oetjen, Rebecca Csomos, John Wilkinson, Brian Rudd, Claudia Benjamim, Steven L. Kunkel, Nicholas Lukacs and Colin Duckett.

- Presenting author: Keystone Symposium, Cell Death and Cellular Senescence, Breckenridge, Colorado, Feb 7-12, 2008 (abstract and poster). “Innate immune responses to lipopolysaccharide require c-IAP1,” Karolyn Oetjen, Rebecca Csomos, John Wilkinson, Brian Rudd, Claudia Benjamim, Steven L. Kunkel, Nicholas Lukacs and Colin Duckett.

- Contributing author: Keystone Symposium, Cell Death and Cellular Senescence, Breckenridge, Colorado, Feb 7-12, 2008 (abstract and poster). “Analysis of XIAP in a murine model of human X-linked lymphoproliferative syndrome: susceptibility to γ-herpesvirus infection,” Julie M. Rumble,

Karolyn A. Oetjen, Casey W. Wright, Paul Stein, Pamela L. Schwartzberg, Beth B. Moore and Colin S. Duckett.

- Presenting author: Era of Hope Meeting, Baltimore, MD, June 2008 (abstract and poster). “The Role of X-linked Inhibitor of Apoptosis in Breast Cancer Development and Progression,” Karolyn A. Oetjen, Stefanie Galban, Julie M. Rumble, Casey W. Wright, Clara Hwang, David Kosoff and Colin S. Duckett.

- Contributing author: Hwang C, Oetjen KA, Kosoff D, Wojno KJ, Albertelli MA, Dunn RL, Robins DM, Cooney KA and Duckett CS. X-linked inhibitor of apoptosis deficiency in the TRAMP mouse prostate cancer model. *Cell Death Differ* 2008, 15:831-840.

- Contributing author: Csomos RA, Wright CW, Galban S, Oetjen KA and Duckett CS. Two distinct signalling cascades target the NF-κB regulatory factor c-IAP1 for degradation. *Biochem J, in press* (2009).

- Contributing author: Galban S, Hwang C, Rumble JM, Oetjen KA, Wright CW, Boudreault A, Durkin J, Gillard JW, Jaquith JB, Morris SJ and Duckett CS. Cytoprotective effects of IAPs revealed by a small molecule antagonist. *Biochem J* 2009, 417:765-771.

- Manuscript in review: Oetjen KA, Wilkinson JC, Benjamim CF, Kunkel SL, Duckett CS and Lukacs NW. Cellular inhibitor of apoptosis protein c-IAP1 contributes to systemic cytokine production during septic shock. *Am J Pathol.*

- Manuscript in submission: Rumble JM, Oetjen KA, Stein P, Schwartzberg PL, Moore BB and Duckett CS. Distinct functional and biochemical properties of XIAP and SAP, two factors targeted in X-linked Lymphoproliferative Syndrome (XLP).

- Dissertation: Contributions to inflammation and sepsis by Inhibitor of Apoptosis proteins. Karolyn Ann Oetjen, Molecular and Cellular Pathology Graduate Program, University of Michigan (2009).

- Fulfillment of the requirements of Ph.D. in the University of Michigan (Molecular and Cellular Pathology Graduate Program), 2009.

- Development of lentiviral vectors that have been requested by and distributed to other laboratories interested in the role of XIAP during tumorigenesis.

Conclusion

XIAP has been identified as a potential target for breast cancer therapeutics, but the specific functions of XIAP that contribute to breast cancer development or progression remain unknown. The major tasks for this phase of this project involved evaluating breast cancer cell lines depleted in XIAP expression in tumor growth models *in vivo* and anchorage-independent growth models *in vitro*. Surprisingly, XIAP did not affect cancer cell growth in these models, and cell lines with rescued expression of XIAP did not demonstrate increased tumorigenesis compared to XIAP-deficient cells. These cell lines have been evaluated for sensitivity to apoptotic stimuli, and XIAP was a necessary anti-apoptotic molecule in these cells and required caspase-inhibitory residues D148 and W310 for this activity. This knowledge will be valuable to guide the development of therapeutics that target XIAP, which are currently in phase I/II clinical trials.

References

Daniel VC, Marchionni L, Hierman JS, Rhodes JT, Devereux WL, Rudin CM, Yung R, Parmigiani G, Dorsch M, Peacock CD and Watkins DN. A Primary Xenograft Model of Small-Cell Lung Cancer Reveals Irreversible Changes in Gene Expression Imposed by Culture In vitro. *Cancer Res, in press.* (2009)

Dean E, Jodrell D, Connolly K, Danson S, Jolivet J, Durkin J, Morris S, Jowle D, Ward T, Cummings J, Dickinson G, Aarons L, Lacasse E, Robson L, Dive C and Ranson M. Phase I trial of AEG35156 administered as a 7-day and 3-day continuous intravenous infusion in patients with advanced refractory cancer. *J Clin Oncol*, 27:1660-1666. (2009)

Galban S, Hwang C, Rumble JM, Oetjen KA, Wright CW, Boudreault A, Durkin J, Gillard JW, Jaquith JB, Morris SJ and Duckett CS. Cytoprotective effects of IAPs revealed by a small molecule antagonist. *Biochem J*, 417:765-771. (2009)

Hwang C, Oetjen KA, Kosoff D, Wojno KJ, Albertelli MA, Dunn RL, Robins DM, Cooney KA and Duckett CS. X-linked inhibitor of apoptosis deficiency in the TRAMP mouse prostate cancer model. *Cell Death Differ*, 15:831-840. (2008)

LaCasse EC, Cherton-Horvat GG, Hewitt KE, Jerome LJ, Morris SJ, Kandimalla ER, Yu D, Wang H, Wang W, Zhang R, Agrawal S, Gillard JW and Durkin JP. Preclinical Characterization of AEG35156/GEM 640, a Second-Generation Antisense Oligonucleotide Targeting X-Linked Inhibitor of Apoptosis. *Clinical Cancer Research* 12: 5231-5241. (2006)

Lewis J, Burstein E, Reffey SB, Bratton SB, Roberts AB and Duckett CS. Uncoupling of the signaling and caspase-inhibitory properties of X-linked inhibitor of apoptosis. *J Biol Chem* 279:9023-9. (2004)

McManus DC, Lefebvre CA, Cherton-Horvat G, St-Jean M, Kandimalla ER, Agrawal S, Morris SJ, Durkin JP and Lacasse EC. Loss of XIAP protein expression by RNAi and antisense approaches sensitizes cancer cells to functionally diverse chemotherapeutics. *Oncogene* 23:8105-17. (2004)

Ravi R, Fuchs EJ, Jain A, Pham V, Yoshimura K, Prouser T, Jalla S, Zhou X, Garrett-Mayer E, Kaufmann SH, Schulick RD, Pardoll DM and Bedi A. Resistance of cancers to immunologic cytotoxicity and adoptive immunotherapy via X-linked inhibitor of apoptosis protein expression and coexisting defects in mitochondrial death signaling. *Cancer Res*, 66:1730-1739. (2006)

Appendices

Appendix 1: Figures 1-9 referenced in the body text.

Appendix 2: Reprints of Hwang *et. al.* 2008 and Galban *et. al.* 2009, referenced in the body text and key reportable outcomes.

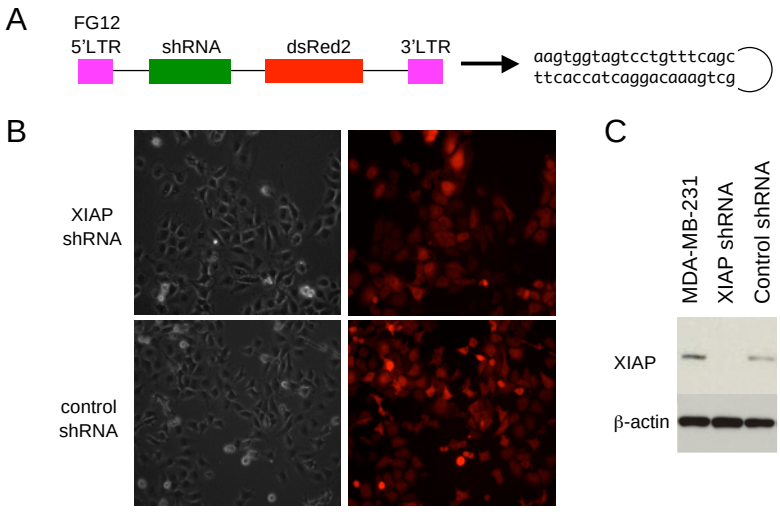

Figure 1. Stable suppression of XIAP in human breast carcinoma cells by RNAi. (A) A short hairpin sequence targeting XIAP (or control hairpin) was cloned into the bicistronic lentiviral vector FG12. Virus was packaged in 293T cells, and MDA-MB-231 cells were infected with viral supernatant. (B) Effective transduction of the lentivirus was confirmed by fluorescence microscopy. Light microscopic images are included for reference. (C) XIAP expression was evaluated by Western blot in parental MDA-MB-231 cells (left) and MDA-MB-231 cells transduced with XIAP shRNA (middle) or control shRNA (right). β-actin is included to control for protein loading (bottom).

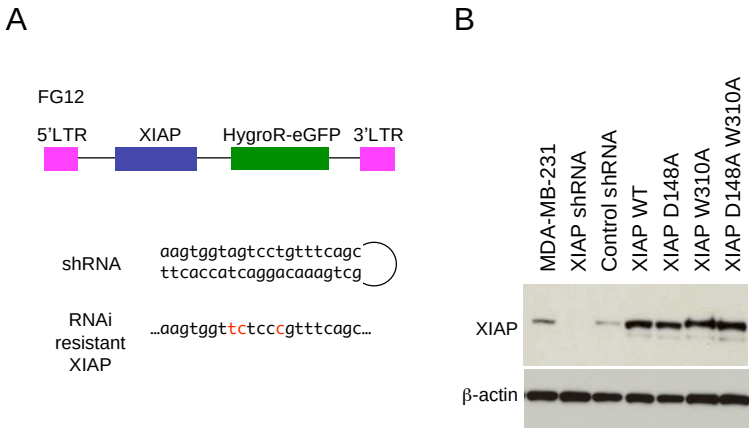

Figure 2. Re-expression of XIAP in shXIAP-expressing MDA-MB-231 cells. (A) Silent mutations were generated in the shRNA-targeted sequence of XIAP cDNA to create constructs resistant to RNAi-mediated suppression. Additional mutations at D148, W310 and H467A were also cloned, and the constructs were expressed using the FG12 lentiviral system. (B) Transduced MDA-MB-231 shXIAP cells were examined for XIAP expression by Western blot.

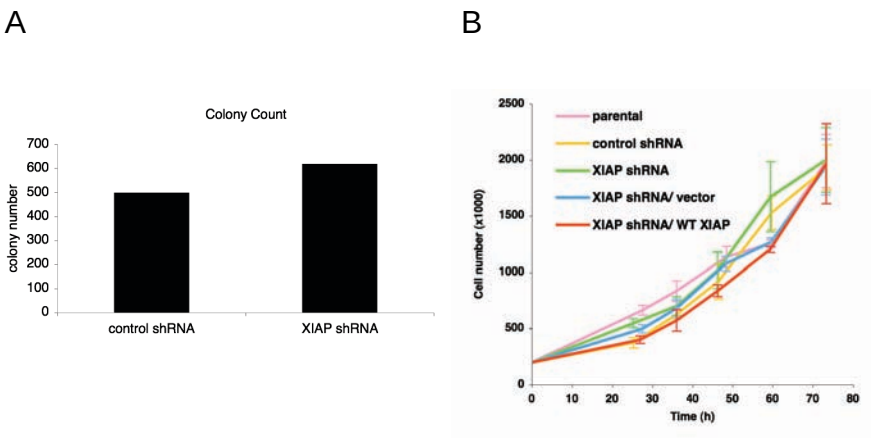

Figure 3. Loss of XIAP in breast carcinoma cells *in vitro.* (A) MDA-MB-231 cells were plated in soft agar, and media was replenished as needed. Foci formation was monitored for 4-6 weeks by fluorescence microscopy. (B) Identical numbers of MDA-MB-231 cells were plated in RPMI with full serum, and cell quantity was measured over three days.

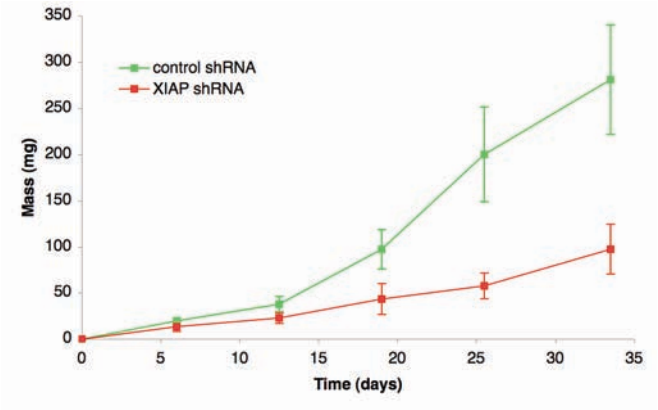

Figure 4. Xenograft tumor growth of XIAP-deficient breast cancer cells. Athymic nude mice were subcutaneously injected with $3x10^6$ MDA-MB-231 cells in 100µL PBS bilaterally, and tumor growth was monitored by two perpendicular caliper measurements over 6 wks. Tumor mass was estimated as $a^2*b/2$, where a<b. Error bars are SEM.

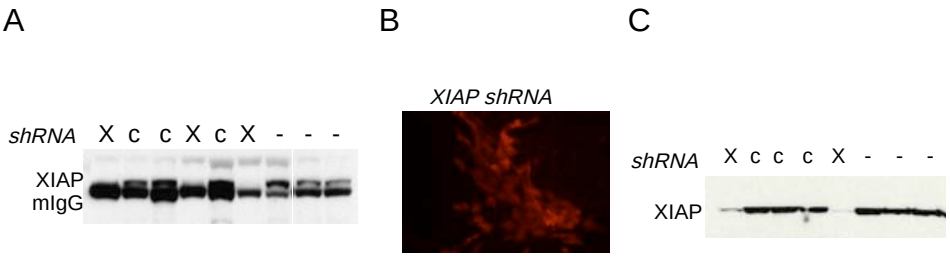

Figure 5. Xenograft tumor expression of XIAP. (A) Lysates of tumor specimens were probed with XIAP mouse monoclonal antibody by Western blot to confirm persistent knock-down of XIAP. Abbreviations for samples: X=XIAP shRNA, c= control shRNA, - = parental MDA-MB-231 cells. (B) Cells from tumor explants were sub-cultured *ex vivo*. Expression of dsRed2 marker in cultures from XIAP shRNA tumors was verified by fluorescent microscopy. (C) *Ex vivo* cultures of tumor cells were lysed and analyzed for XIAP expression by Western blot. Abbreviations as in (A).

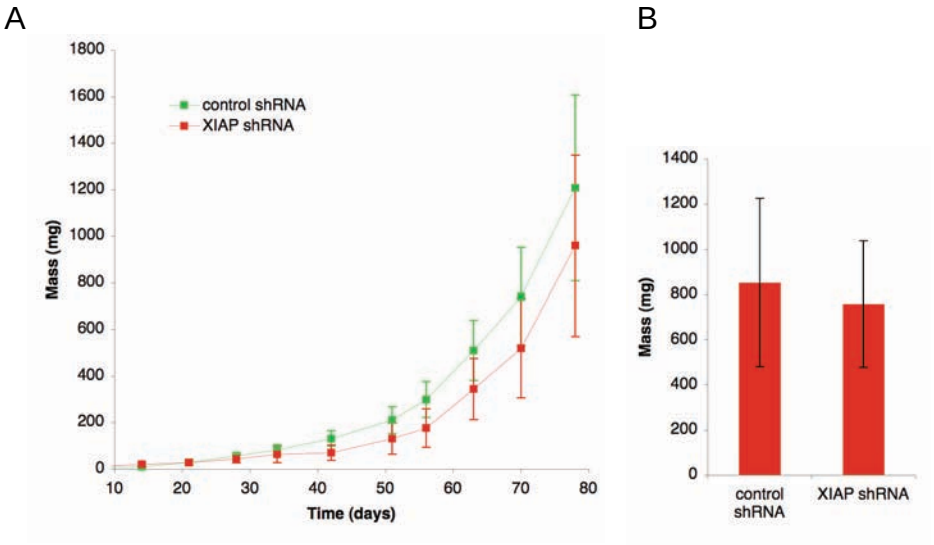

Figure 6. Xenograft tumor growth of an independently derived XIAP-deficient breast cancer cell line. Athymic nude mice were subcutaneously injected with $3x10^6$ MDA-MB-231 cells in 100µL PBS bilaterally. (A) Tumor growth was monitored by two perpendicular caliper measurements over 6 weeks. Tumor mass was estimated as $a^2*b/2$, where a<b. (B) Tumors were excised from euthanized mice on day 78, and tumor mass was measured. Error bars are SEM in each panel.

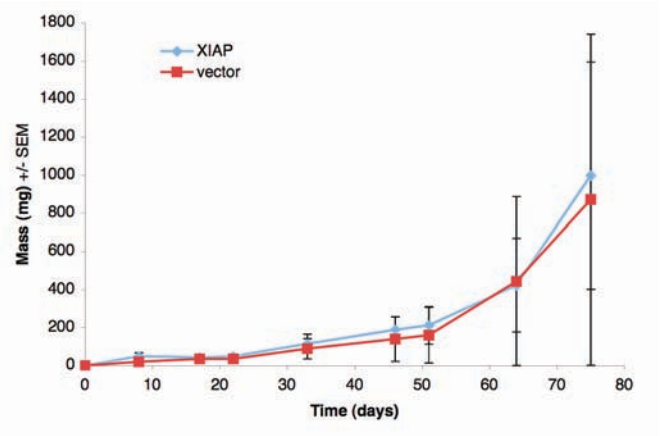

Figure 7. Xenograft tumor growth following re-expression of XIAP in XIAP-deficient breast cancer cells. Athymic nude mice were subcutaneously injected with $3x10^6$ MDA-MB-231 cells in 100µL PBS bilaterally, and tumor growth was monitored by two perpendicular caliper measurements over 6 wks. Tumor mass was estimated as $a^2*b/2$, where a<b. Error bars are SEM.

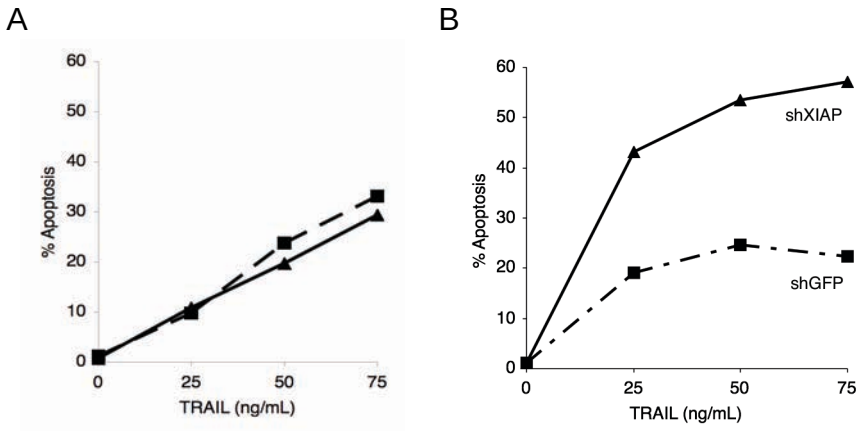

Figure 8. XIAP-dependent sensitivity to TRAIL. (A) MDA-MB-231 cells expressing shXIAP (solid) or control shRNA (dash) were treated with TRAIL for 2 hours and analyzed by flow cytometry for propidium iodide-positive cells immediately after treatment. (B) Cells were treated as before and analyzed 48 hours after treatment.

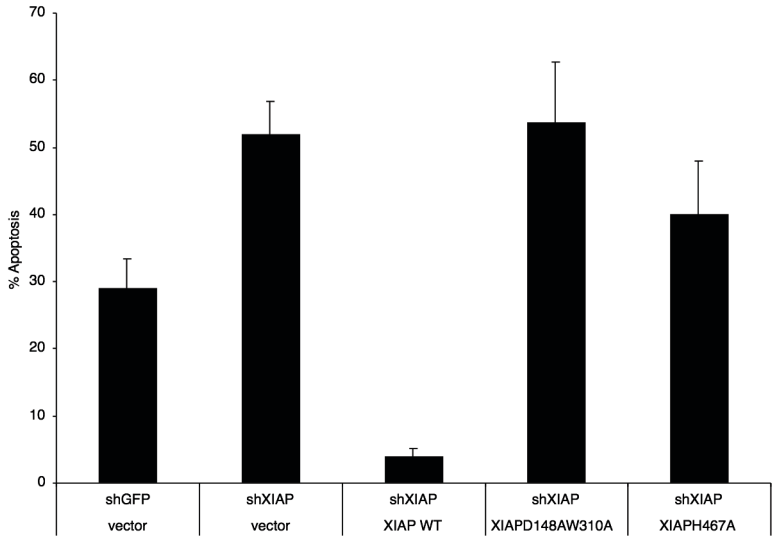

Figure 9. TRAIL-induced apoptosis in XIAP-mutant expressing breast cancer cell lines. MDA-MB-231 cells expressing XIAP shRNA plus RNAi-resistant XIAP mutants were treated with TRAIL for 2 hours and analyzed by flow cytometry for propidium iodide-positive cells 48 hours after treatment.

Cell Death and Differentiation (2008) 15, 831–840

www.nature.com/cdd

X-linked inhibitor of apoptosis deficiency in the TRAMP mouse prostate cancer model

C Hwang[1,5], KA Oetjen[2,5], D Kosoff[2], KJ Wojno[3], MA Albertelli[4], RL Dunn[3], DM Robins[4], KA Cooney[1,3] and CS Duckett*[,1,2]

Deregulation of apoptotic pathways plays a central role in cancer pathogenesis. X-linked inhibitor of apoptosis protein (XIAP), is an antiapoptotic molecule, whose elevated expression has been observed in tumor specimens from patients with prostate carcinoma. Studies in human cancer cell culture models and xenograft tumor models have demonstrated that loss of XIAP sensitizes cancer cells to apoptotic stimuli and abrogates tumor growth. In view of these findings, XIAP represents an attractive antiapoptotic therapeutic target for prostate cancer. To examine the role of XIAP in an immunocompetent mouse cancer model, we have generated transgenic adenocarcinoma of the mouse prostate (TRAMP) mice that lack XIAP. We did not observe a protective effect of *Xiap* deficiency in TRAMP mice as measured by tumor onset and overall survival. In fact, there was an unexpected trend toward more aggressive disease in the *Xiap*-deficient mice. These findings suggest that alternative mechanisms of apoptosis resistance are playing a significant oncogenic role in the setting of *Xiap* deficiency. Our study has implications for XIAP-targeting therapies currently in development. Greater understanding of these mechanisms will aid in combating resistance to XIAP-targeting treatment, in addition to optimizing selection of patients who are most likely to respond to such treatment.
Cell Death and Differentiation (2008) **15,** 831–840; doi:10.1038/cdd.2008.15; published online 8 February 2008

Apoptosis is a process of cell death that is tightly regulated by a cadre of both pro- and antiapoptotic proteins. In contrast to healthy cells, a hallmark of cancerous cells is the acquired capacity to evade this process of programmed cell death.[1,2] The acquisition of genetic lesions leading to oncogene activation normally triggers a program of apoptosis or senescence. Additionally, the tumor microenvironment often exposes malignant cells to apoptotic stimuli, such as hypoxia or activation of death receptors. Thus, suppression of the pathway leading to cell death has been suggested as a necessarily early event in the development of neoplasia.

Execution of the apoptotic cell death process is carried out by caspases, a family of cysteine aspartate proteases.[3,4] During apoptosis, loss of mitochondrial integrity or engagement of death receptors leads to the activation of initiator caspase-9 or -8, respectively. In either case, the initiator caspases cleave and activate effector caspases, including caspase-3 or -7. The cascade of caspase cleavage is regulated by X-linked inhibitor of apoptosis protein (XIAP). XIAP belongs to the IAP family, characterized by containing at least one zinc-binding baculovirus IAP repeat.[5] The only member of the IAP family that potently inhibits caspase activity, XIAP has been demonstrated to directly inhibit caspases-3, -7 and -9, blocking both intrinsic and extrinsic apoptotic signals.[6] Given its role in apoptosis, there has been much interest in understanding the role of XIAP in cancer and evaluating XIAP as a therapeutic target.[7–9]

XIAP overexpression has been reported in a variety of human cancers.[10–16] Increased XIAP levels have been linked to escaping anoikis and apoptosis induced by radiation, chemotherapy and death receptor ligands.[13,17–22] Furthermore, antagonism of XIAP has been reported to have antitumor activity in a number of models, including prostate cancer.[21,23–25] Consistent with an antiapoptotic role, high levels of XIAP have an adverse prognosis in certain cancers.[14,15] However, there was an unexpected favorable prognosis seen in prostate and non-small cell lung cancers with high levels of XIAP expression.[12,26]

We thus chose to further examine the role of XIAP in a tumor model that would resemble human cancer more closely than xenograft or *in vitro* studies. In this study, we describe an evaluation of prostate cancer development in the presence and absence of XIAP using the transgenic adenocarcinoma of the mouse prostate (TRAMP) model. Prostate-specific expression of SV40 T-antigen in TRAMP mice results in 100% penetrance of prostate tumors and a substantial proportion with metastatic disease.[27] XIAP expression is elevated in TRAMP tumors compared to normal prostate epithelium,[12] further justifying an evaluation of the effect of *Xiap* deficiency in this model.

[1]Department of Internal Medicine, University of Michigan Medical School, Ann Arbor, MI, USA; [2]Department of Pathology, University of Michigan Medical School, Ann Arbor, MI, USA; [3]Department of Urology, University of Michigan Medical School, Ann Arbor, MI, USA and [4]Department of Human Genetics, University of Michigan Medical School, Ann Arbor, MI, USA
*Corresponding author: CS Duckett, Department of Pathology and Internal Medicine, University of Michigan, BSRB, Room 2057, 109 Zina Pitcher Place, Ann Arbor, MI 48109-2200, USA. Tel.: +734 615 6414; Fax: +734 763 2162; E-mail: colind@umich.edu
[5]These authors contributed equally to this work.
Keywords: XIAP; BIRC4; prostate cancer
Abbreviations: c-IAP1, cellular inhibitor of apoptosis protein 1; c-IAP2, cellular inhibitor of apoptosis protein 2; IAP, inhibitor of apoptosis protein; MRI, magnetic resonance imaging; PIN, prostatic intraepithelial neoplasia; RIAP, rodent inhibitor of apoptosis protein; TRAMP, transgenic adenocarcinoma of mouse prostate; TUNEL, terminal dUTP nick end labeling; XIAP, X-linked inhibitor of apoptosis protein
Received 12.9.07; revised 20.12.07; accepted 07.1.08; Edited by A Villunger; published online 08.2.08

Surprisingly, we found no evidence for a protective effect of *Xiap* deficiency in TRAMP mice. *Xiap*-deficient mice demonstrated no difference in tumor onset or overall survival compared to controls. Furthermore, tumor histology revealed similar patterns of differentiation and frequencies of apoptosis and proliferation in tumors from both groups. To our knowledge, these experiments represent the first examination of XIAP in an immunocompetent cancer model and differ markedly from previously published studies using xenografted cell lines. These results are relevant to the development of therapeutics, currently in clinical trials, that specifically antagonize XIAP.

Results

Loss of XIAP in TRAMP mice does not prevent tumor development or improve survival. *Xiap*-deficient TRAMP mice were generated with the hypothesis that mice deficient in XIAP may be protected from tumor formation compared to wild-type controls. Prostate size was monitored by magnetic resonance imaging (MRI). Representative MRI images from two littermate pairs of TRAMP mice are shown in Figure 1. In the first pair, tumor onset occurred sooner in the *Xiap*-deficient mouse compared to its wild-type littermate, but there was no appreciable difference in tumor onset or growth in the second littermate pair. Aggregate Kaplan–Meier analysis showed no difference between the two groups of mice (data not shown). The median age of tumor onset was 25.9 weeks for *Xiap*-deficient mice and 25.6 weeks for wild-type mice (*Xiap*-deficient mice $n=9$; wild-type mice $n=8$; $P=0.88$).

In addition to MRI, tumor onset was evaluated by abdominal palpation. The median age at the time of palpable tumor onset was 26.0 weeks in *Xiap*-deficient mice and 27.3 weeks in littermate controls (*Xiap*-deficient mice $n=13$; wild-type mice $n=11$). Kaplan–Meier analysis was used to compare the

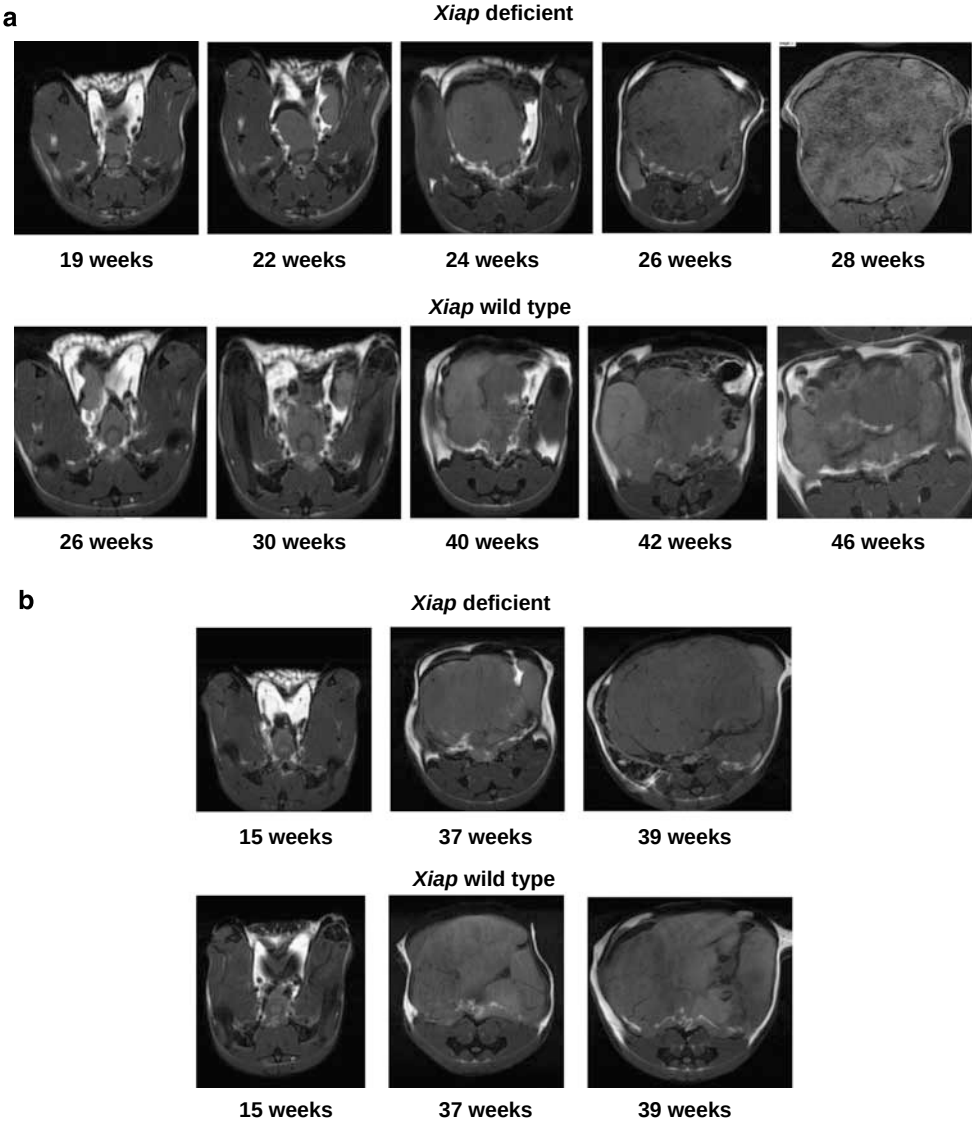

Figure 1 MRI images of prostate tumors in *Xiap*-deficient and wild-type TRAMP mice. MRI scans are shown for two representative pairs (**a**, **b**) of *Xiap*-deficient and wild-type TRAMP mice

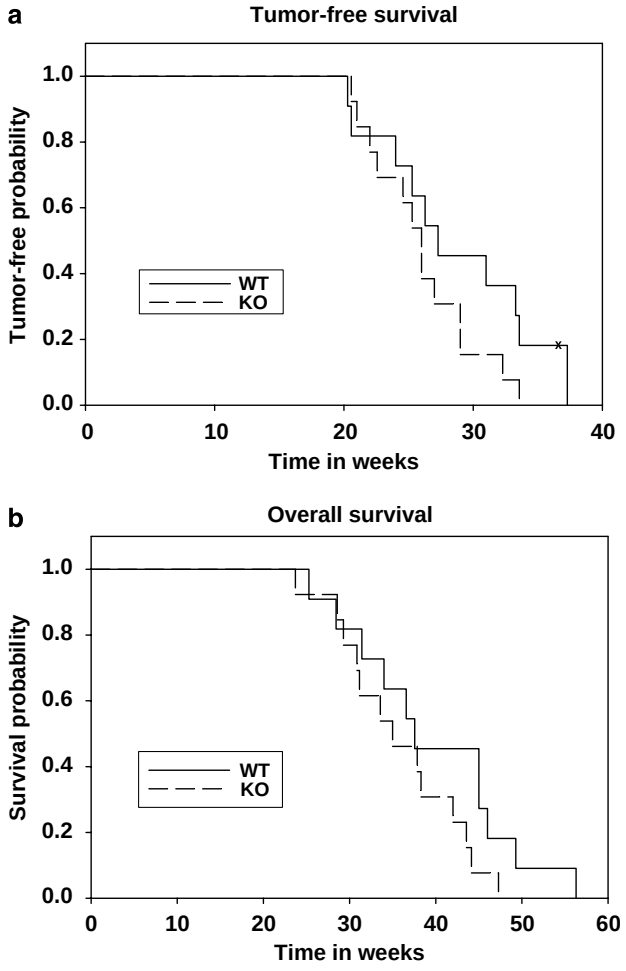

Figure 2 Kaplan–Meier analysis for tumor onset and overall survival. (**a**) Kaplan–Meier curves were plotted for *Xiap*-deficient (dotted line) and wild-type (solid line) TRAMP mice. The probability of remaining without tumor is plotted against age in weeks. One wild-type TRAMP mouse died from unknown causes at 36 weeks of age before evidence of tumor onset, and this mouse (x) was censored. A one-sided log-rank analysis yields a *P*-value of 0.924, indicating a 7.6% probability that *Xiap*-deficient mice would protect against tumor onset. (**b**) Kaplan–Meier curves were plotted for *Xiap*-deficient (dotted line) and wild-type (solid line) TRAMP mice. The probability of survival is plotted against age in weeks. A one-sided log rank analysis yields a *P*-value of 0.928, indicating a 7.2% probability that *Xiap* deficiency is protective for overall survival

probability of remaining without tumor between the two groups (Figure 2a). There was no evidence for a protective effect of *Xiap* deficiency in TRAMP mice. In fact, there was an unexpected trend for the *Xiap*-deficient mice to develop tumors earlier than wild-type controls, although the difference was not statistically significant (two-sided *P*-value = 0.15).

Although *Xiap* deficiency did not alter TRAMP tumor onset, inhibition of apoptosis by XIAP could contribute to a more lethal phenotype later in tumor progression. However, there was no evidence for a protective effect of *Xiap* deficiency in TRAMP mice on overall survival, and the trend for poorer outcome in the *Xiap*-deficient mice was again observed (Figure 2b). The median age at time of death was 35.0 weeks for *Xiap*-deficient TRAMP mice ($n = 13$), and the median age of control TRAMP mice at the time of death was 37.6 weeks ($n = 11$), but this difference was not statistically significant (two-sided *P*-value = 0.15).

***Xiap* deficiency does not retard growth of TRAMP tumors.** Since apoptosis may affect tumor growth without significantly impacting either tumor onset or overall survival, we hypothesized that a deficiency in XIAP may be expected to result in a decreased tumor burden. To assess tumor burden, the mass of the primary tumor at the time of necropsy was determined and tumor mass as a percentage of the mass of the mouse at necropsy was calculated. By both of these measures, *Xiap* deficiency did not result in a decrease in tumor burden as compared to wild-type controls (Figure 3a). Indeed, average tumor mass was somewhat greater in *Xiap*-deficient TRAMP mice (11.1 ± 5.06 g) than littermate controls (9.05 ± 4.78 g) despite the shortened survival observed above.

Although an effect on tumor burden at the time of death was not seen, tumor size may reflect the duration of growth as opposed to tumor growth rate. Thus, the time from palpable tumor to time of killing was measured. Generally, a prolonged duration between tumor onset and killing would indicate slower tumor growth. However, when *Xiap*-deficient TRAMP mice were compared to controls, there was no delay from the time of palpable tumor to time of killing (Figure 3b, last bars). As previously noted, the time to palpable tumor and time to death for *Xiap*-deficient TRAMP mice was shorter than controls.

Tumor growth was also assessed over time by clinical examination on a four-point scale. The time from palpable tumor to larger tumors was calculated and compared between *Xiap*-deficient TRAMP mice and controls. In agreement with our previous finding that *Xiap* deficiency does not delay time to killing or time from palpable tumor to killing, tumors in *Xiap*-deficient mice did not grow more slowly than tumors in controls (Figure 3c). To the contrary, the average time from palpable tumor to larger tumors (size 3 or 4) was seen to be shorter in *Xiap*-deficient mice.

***Xiap* deficiency does not result in less aggressive TRAMP tumors.** When tumor mass at autopsy was measured, it was observed that the mass of the primary tumor varied significantly, indicating that local growth did not always correspond to tumor lethality. Tumor aggressiveness also correlates with tumor grade and metastatic potential. Elevated expression of XIAP has been observed to correlate with higher tumor grades in renal cell carcinoma and breast cancer,[10,14] although this is not the case in other cancers.[26,28] To evaluate the effect of *Xiap* deficiency on tumor grade, tumor differentiation was assessed as another measure of tumor aggressiveness. Poorly and moderately differentiated carcinomas, as well as the more benign phylloides tumor, were observed in both *Xiap*-deficient and wild-type TRAMP mice. Examples of poorly differentiated and moderately differentiated primary tumors in both *Xiap*-deficient and wild-type mice are shown in Figure 4a. When tabulated, 67% (6/9) *Xiap*-deficient mice were noted to have carcinoma and the remainder (33%, 3/9) were phylloides. In comparison, 50% (4/8) of tumors from control mice were carcinoma and 50% (4/8) were phylloides. Among those

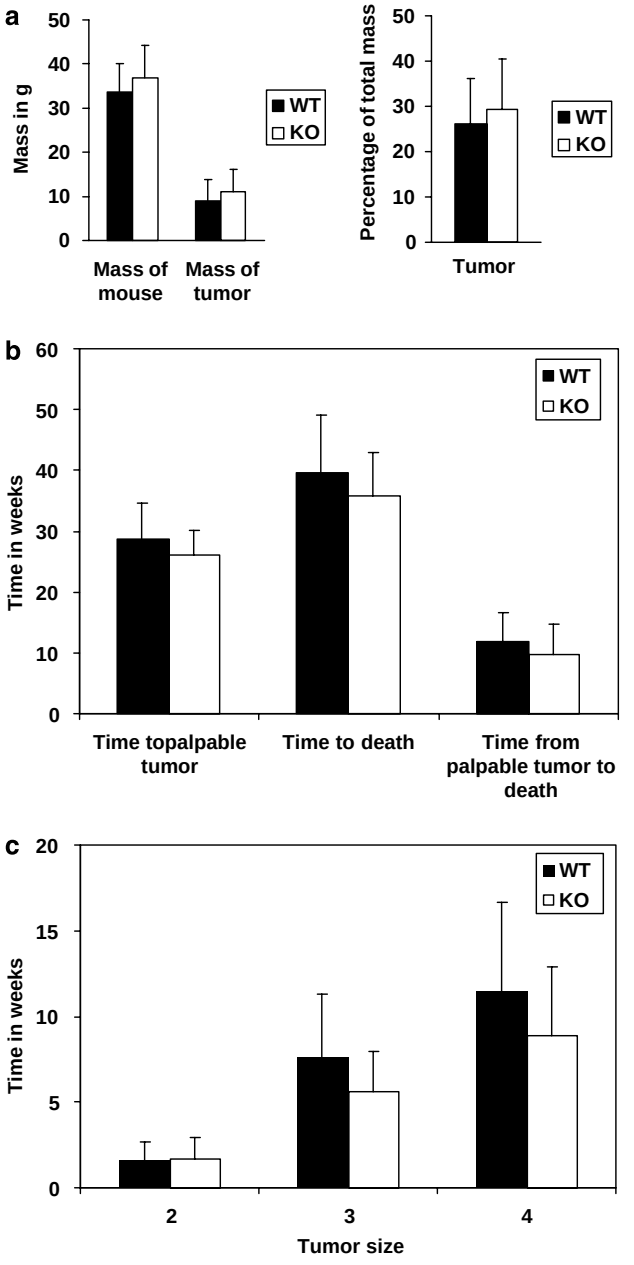

Figure 3 Comparison of tumor characteristics in *Xiap*-deficient and wild-type TRAMP mice. (**a**) Mass of animals and mass of tumors at necropsy were compared between the wild-type and *Xiap*-deficient mice. The tumor mass as a percentage of total mouse mass at the time of necropsy was also compared. Mean values are plotted with error bars representing one standard deviation. (**b**) Time to palpable tumor, time to death and time from palpable tumor to death were assessed for *Xiap*-deficient and wild-type mice. Mean values for each variable are plotted with error bars representing one standard deviation. (**c**) The time in weeks from tumor onset (size 1) to larger tumors (sizes 2–4) was calculated for each cohort of mice. Mean values for each variable are plotted with error bars representing one standard deviation

classified as carcinoma, tumors were poorly differentiated in 83% of *Xiap*-deficient mice (5/6 mice with carcinoma) and 50% of controls (2/4 mice with carcinoma). Overall, this equated to 56% of the entire cohort of *Xiap*-deficient mice with poorly differentiated carcinoma and 25% of the wild-type cohort (Figure 4b). Therefore, *Xiap*-deficient mice are not protected from more aggressive histologic subtypes of TRAMP tumors.

Xiap-deficient and control TRAMP mice were also evaluated for metastatic spread of tumor. An increase in XIAP has been implicated in resistance to anoikis and increased metastatic potential.[17,20] However, at necropsy, both *Xiap*-deficient and wild-type mice were observed to have pelvic nodal metastases and distant metastases. Metastatic deposits were confirmed histologically and representative images are presented in the right-hand panels of Figure 4a. When quantified, 56% (5/9) of *Xiap*-deficient TRAMP mice were noted to have metastases compared to 63% (5/8) of control TRAMP mice (Figure 4b). Evidence of distant metastases (liver and lung) was identified in three *Xiap*-deficient TRAMP mice (33%, 3/9 mice) compared to two control mice (25%, 2/8 mice). Thus, *Xiap*-deficient mice were not protected from metastatic spread. The majority of metastatic lesions in both *Xiap*-deficient and control TRAMP mice were poorly differentiated.

***Xiap* deficiency does not result in decreased incidence of pre-invasive lesions.** Elevation of XIAP expression has been observed in pre-invasive prostatic intraepithelial neoplasia (PIN) specimens from patients treated for prostate cancer as well as TRAMP mice.[12] To investigate the possibility that XIAP contributes to early tumor development, we studied the effect of loss of XIAP in a cohort of *Xiap*-deficient and control TRAMP mice who were followed until 25 weeks of age. Mice were assessed for prostate gland histology and micrometastatic disease (Table 1). None of the 25-week-old mice had evidence of micrometastases. There was no difference between *Xiap*-deficient and wild-type TRAMP mice in the incidence of PIN or microscopic carcinoma.

Loss of XIAP does not affect apoptosis or proliferation of tumor cells *in vivo*. Because of the accepted role of XIAP in cell death, we examined tumor specimens from *Xiap*-deficient mice by terminal dUTP nick end labeling (TUNEL) staining to assess the number of cells undergoing apoptosis (Figure 5a). There was no difference seen in TUNEL staining between the *Xiap*-deficient and wild-type tumors. Moreover, when quantitated, the apoptotic index was not increased in *Xiap*-deficient compared to wild-type TRAMP tumors (Figure 5b). In most tumors from both wild-type and *Xiap*-deficient TRAMP mice, the apoptotic index was on the order of 10 apoptotic cells per 1000, with only a few tumors exhibiting higher apoptotic indices. There did not seem to be a correlation between apoptotic index and histologic subtype. Of the three tumors with apoptotic indices greater than 15 cells per 1000, one was poorly differentiated, one was well differentiated and one was phylloides.

In view of previous work in resected lung cancer suggesting an increased proliferative and mitotic index in tumors with low XIAP expression,[26] we also performed an analysis of the proliferative rates present in these TRAMP tumors. Using both nuclear Ki-67 staining and mitotic figures as markers for proliferation, we did not observe any differences between the wild-type and *Xiap*-deficient TRAMP tumors (Figure 6).

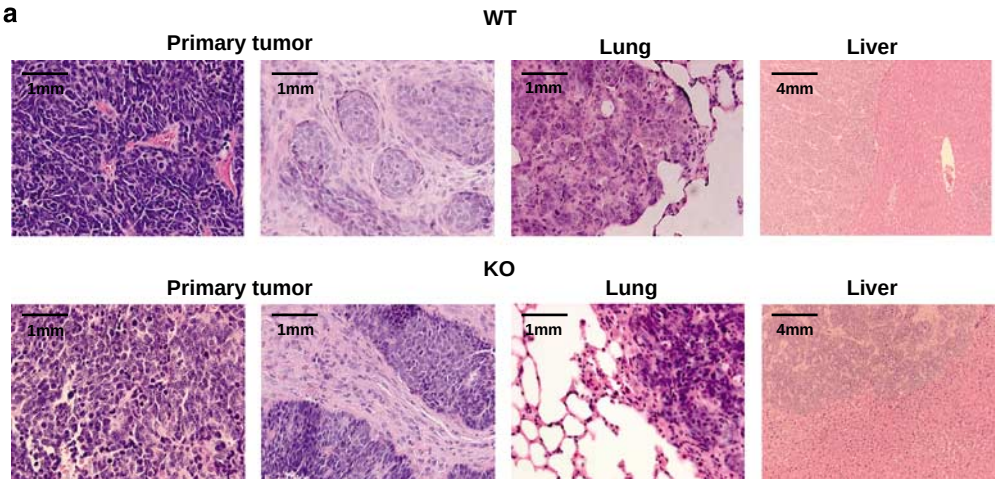

b

	Wild type	Knockout	*P*-value
Primary tumor			
Phylloides	4/8 50%	3/9 33%	0.49
Carcinoma	4/8 50%	6/9 67%	0.49
Poorly Differentiated	2/8 25%	5/9 56%	0.20
Moderately Differentiated	1/8 13%	1/9 11%	0.87
Well Differentiated	1/8 13%	0/9 0%	0.27
Metastases			
Mice with Metastases	5/8 63%	5/9 56%	0.77
Poorly Differentiated	4/8 50%	5/9 56% *	0.82
Moderately Differentiated	1/8 13%	1/9 11% *	0.93
Mice with distant metastases	2/8 25%	3/9 33%	0.71
Liver	1/8 13%	3/9 33%	0.31
Lung	2/8 25%	1/9 11%	0.45

*one mouse had separate metastases with poor and well-differentiated histology

Figure 4 Histology from primary and metastatic lesions of *Xiap*-deficient and wild-type TRAMP mice. (**a**) Examples of poorly differentiated tumors from wild-type and *Xiap*-deficient mice are shown in the left-most panels. Examples of moderately differentiated tumors are shown in the second set of panels. Metastases to liver and lung were also histologically confirmed and representative images are shown in the two right-most panels. (**b**) Results of histologic analysis for both primary and metastatic tumors were tabulated and compared between the wild-type and *Xiap*-deficient mice

Table 1 Histologic analysis of tumors from 25-week-old wild-type and *Xiap*-deficient TRAMP mice

	Wild type (%)	Knockout (%)	*P*-value
Primary tumor			
Phylloides	1/8 (13)	0/8 (0)	0.30
Carcinoma	2/8 (25)	2/8 (25)	1.00
Poorly differentiated	2/8 (25)	1/8 (13)	0.52
Well differentiated	0/8 (0)	1/8 (13)	0.30
PIN	5/8 (63)	6/8 (50)	0.59
Metastases			
Mice with metastases	0/8 (0)	0/8 (0)	1.00

Wild-type and *Xiap*-deficient mice were followed in cohorts of 10 mice until 25 weeks of age; eight of ten total mice were left in both groups at this time. Results from histologic analysis were tabulated and compared.

Finally, lysates from TRAMP tumors were assessed for expression of caspase-9 and the presence of active caspase-3 (Figure 7a). We did not detect any active caspase-3 in either wild-type or *Xiap*-deficient TRAMP tumors. This finding is consistent with our previous finding of generally low apoptotic rates in TRAMP prostate tumors.

***Xiap* deficiency does not increase c-IAP1 and c-IAP2 expression in TRAMP tumors.** Of the mammalian IAP family members, only cellular IAP1 (c-IAP1) and c-IAP2 are capable of binding caspases and might functionally compensate in the apoptotic pathway following loss of XIAP.[29] Furthermore, in the initial description of *Xiap*-deficient mice, it was found that c-IAP1 and c-IAP2 are overexpressed in *Xiap*-deficient mice.[30] For this reason, expression of c-IAP1 and c-IAP2 was examined in prostate tumor specimens from control and *Xiap*-deficient mice by immunoblot (Figure 7a). There was no obvious compensatory overexpression of c-IAP1 or c-IAP2 in the *Xiap*-deficient TRAMP tumors. Detection of c-IAP1 and c-IAP2 by immunoblot was quantified, and results are presented in Figure 7b. Not only was there no evidence of overexpression of c-IAP1 or c-IAP2, the mean level of c-IAP2 was actually decreased in the *Xiap*-deficient tumors compared to wild-type controls. Since levels of c-IAP1 and c-IAP2 are also subject to post-translational regulation,[31] expression of *c-iap1* and *c-iap2* transcripts was also examined by quantitative RT-PCR. Consistent with measurements of protein expression, expression of *c-iap1*

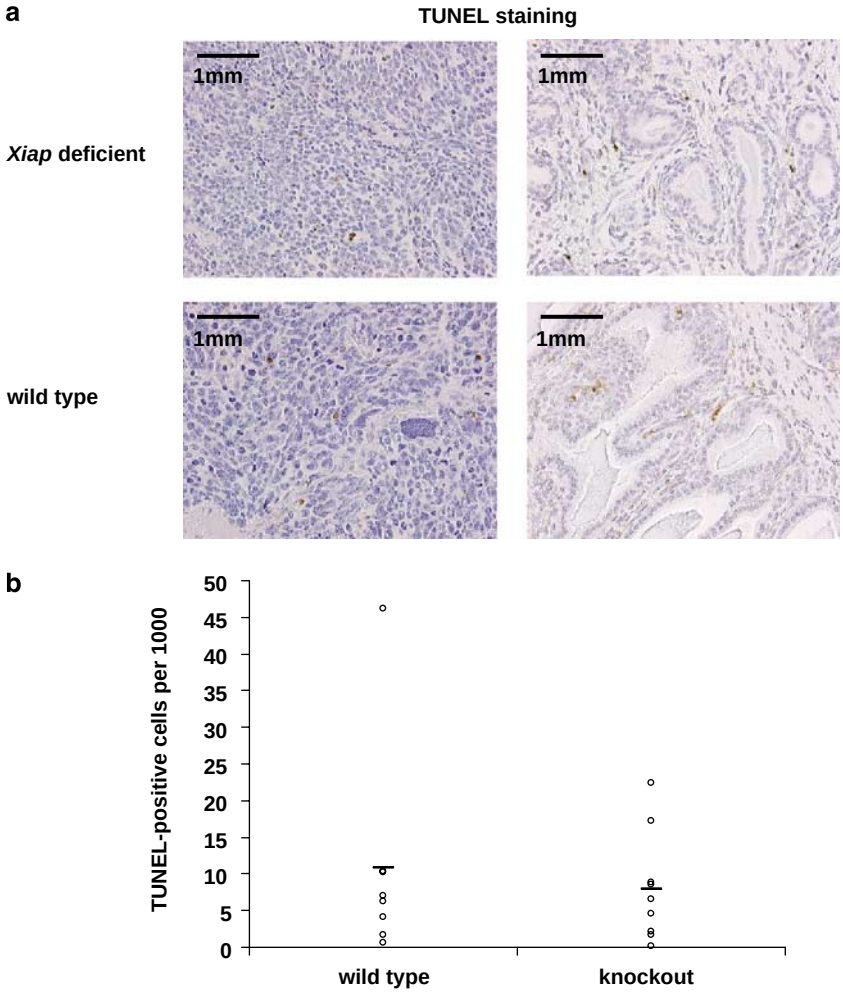

Figure 5 Frequency of apoptotic cells in *Xiap*-deficient tumors. (**a**) Primary prostate tumors were assessed for apoptotic cells using TUNEL staining. Representative images are shown from tumors with poorly differentiated carcinoma (left) and phylloides histology (right). (**b**) The number of TUNEL-positive cells per 1000 total cells was plotted for wild-type and *Xiap*-deficient mice. Mean values are represented by (—)

and *c-iap2* mRNA was not increased in *Xiap*-deficient tumors compared to controls (Figure 7c). Levels of *c-iap1* and *c-iap2* transcripts were actually somewhat less in the *Xiap*-deficient group, which was surprising but correlated with our observations of protein levels. In summary, compensation by c-IAP1 or c-IAP2 could not explain why *Xiap* deficiency did not protect TRAMP mice against tumor onset, growth or lethality.

Discussion

Malignant cells demonstrate a resistance to apoptosis, which allows these cells to survive in cellular environments that would typically induce cell death.[1] One proposed mechanism for the acquired capacity of cancer cells to evade apoptosis is antagonism of caspase activity through increased expression of XIAP. Elevated expression of XIAP has been demonstrated in cancers of various origins.[10–16] Not only is XIAP overexpressed in cancer, increased XIAP expression has been shown to contribute to apoptosis resistance and conversely, XIAP antagonism sensitizes cancer cells to multiple types of apoptotic stimuli *in vitro* and *in vivo*.[13,17–25,28,32–37] These apoptotic stimuli have included various chemotherapeutic agents, ionizing radiation, tumor necrosis factor-related apoptosis-inducing ligand, anoikis induction and immune clearance by cytotoxic lymphocytes. Despite these encouraging reports supporting a role for XIAP in the pathogenesis of cancer, there are data that are difficult to reconcile with the currently known functions of XIAP. Specifically, the paradoxical and dramatic favorable prognostic value of elevated XIAP levels observed in patients with resected prostate cancer does not correspond with the predicted increased resistance to apoptosis.[12] Interestingly, c-IAP1 and c-IAP2 expression correlated negatively with prognosis in this same group of patients.

We report here that *Xiap*-deficient TRAMP mice do not develop tumors later than wild-type TRAMP mice. Furthermore, *Xiap* deficiency does not lessen the lethality, metastatic potential, histologic grade or tumor growth of TRAMP tumors; in fact, the data suggested a trend of more aggressive behavior in *Xiap*-deficient TRAMP tumors. Thus, we conclude that although elevations of XIAP expression have been

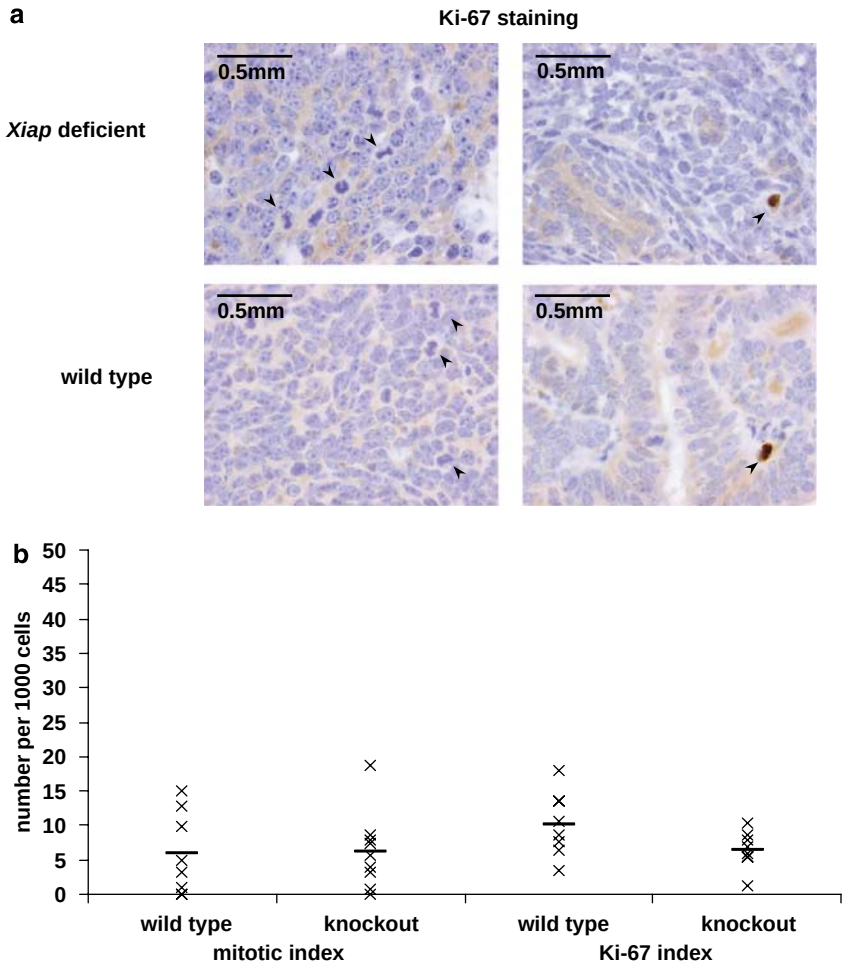

Figure 6 Proliferative indices in *Xiap*-deficient tumors. (**a**) Primary prostate tumors were stained immunohistochemically for Ki-67 (a proliferative marker). Ki-67 proliferative index and mitotic index were calculated. Representative images demonstrating both mitotic figures as well Ki-67-positive cells are shown in the left and right-hand panels, respectively. (**b**) The number of Ki-67-positive cells and the number of mitotic figures per 1000 total cells were plotted for wild-type and *Xiap*-deficient mice. Mean values are represented by (—)

observed in TRAMP tumors, upregulation of XIAP is not essential for transformation of prostate epithelium. It is possible that the aggressiveness of the TRAMP model, in which p53 and pRB are inhibited by the SV40 T-antigen, may have overwhelmed the ability to detect an effect of *Xiap* deficiency. In addition, the inhibition of p53 itself may be sufficient to inhibit apoptosis. However, the TRAMP model has been used to successfully establish a role for the antiapoptotic *Bcl-2* in tumorigenesis,[38] as well as to demonstrate that compounds such as green tea and celecoxib suppress tumorigenesis.[39,40]

These findings suggest that although XIAP is overexpressed in cancer it may not play a causal role in tumor pathogenesis. Conspicuously, evidence of *XIAP* mutations, translocations or amplifications, as is typically associated with classic oncogenes, has been absent in human cancers. Worth considering is the possibility that overexpression of XIAP may instead be a surrogate marker for other biologic behaviors. For example, XIAP is known to be upregulated by hypoxia[32] and thus may be overexpressed in tumors that are outgrowing a vascular supply.

Alternatively, XIAP may modulate apoptosis and tumor progression without being a classic oncogene. In this case, tumor formation in the absence of XIAP could occur if increased apoptosis was compensated by an increase in proliferation. In fact, although Ferreira *et al.*[26] did not observe a correlation between XIAP expression levels and apoptotic index in resected non-small cell lung cancer, they did note an increased proliferative and mitotic index in tumors with low XIAP expression. However, the surprising finding that *Xiap* deficiency did not result in an increase in the apoptotic index suggests that an increased proliferative index would not explain our findings. Indeed, when proliferative rate and mitotic index were assessed, there were no discernible differences between the wild-type and *Xiap*-deficient mice.

In addition, expression of the oncogenic SV40 T-antigen in the absence of XIAP may have selected for pathogenic mechanisms of apoptosis resistance that do not depend on XIAP. This selection pressure may be less acute in a clinical setting when XIAP antagonists are given after cancer has already developed. To explore the possibility of

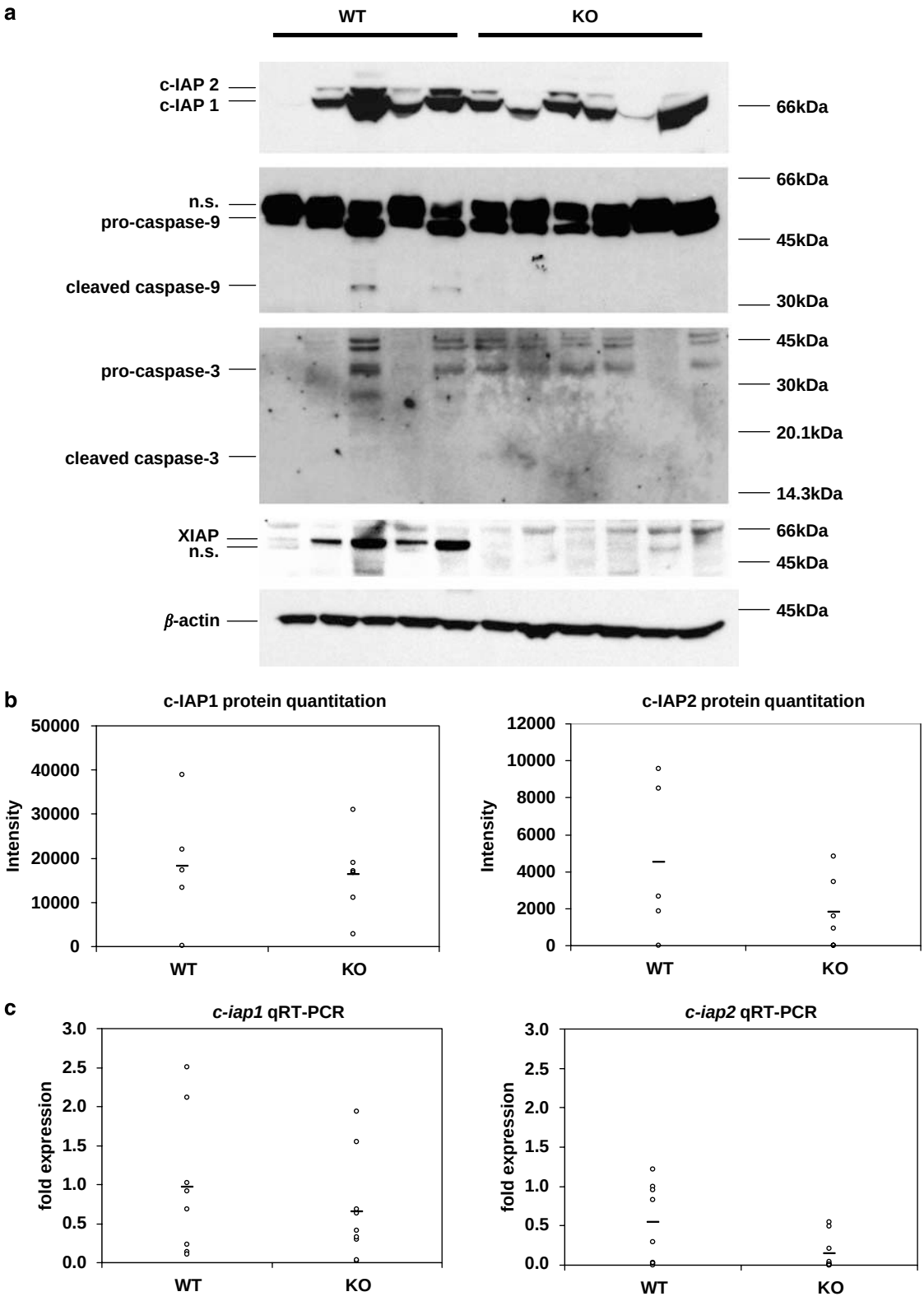

Figure 7 Expression of c-IAP1, c-IAP2 and other apoptotic proteins in Xiap-deficient TRAMP tumor specimens. (**a**) Immunoblot of c-IAP1 and c-IAP2 protein levels in primary tumor lysates. The same lysates were also probed for caspase-3 (full-length 32 kDa, cleaved form 19 or 17 kDa), caspase-9 (full-length 46 kDa, cleaved form 36 kDa) and XIAP (57 kDa). A β-actin immunoblot is shown to demonstrate equal total protein loading. (**b**) Expression levels of c-IAP1 and c-IAP2 protein based on immunoblotting were quantitated using ImageJ software. Relative intensity is plotted on the *y* axis. Mean values are represented by (—). (**c**) Expression of *c-iap1* and *c-iap2* mRNA in tumor specimens, as assessed by quantitative RT-PCR. Fold expression relative to normal prostate is plotted on the *y* axis for wild-type and *Xiap*-deficient cohorts. n.s. nonspecific

XIAP-independent mechanisms of apoptosis inhibition, c-IAP1 and c-IAP2 were evaluated as obvious candidates for a possible compensatory effect. No evidence for such a role was found based on levels of c-IAP1 and c-IAP2 overexpression. Moreover, although c-IAP1 and c-IAP2 are capable of binding caspases, the affinity of c-IAP1 or c-IAP2 for caspases is much lower than XIAP, and recent data suggest that both are incapable of inhibiting caspase activity.[29,41] If inhibition of caspases is relevant to the physiology of cancer cell biology and XIAP overexpression, it is unlikely that c-IAP1 or c-IAP2 can compensate for this activity.

Another possibility for our results is the absence of a significant apoptotic stimulus in our experiments. Although it has been reported that cancer cells can have high basal levels of apoptotic signaling molecules such as caspases-3 and -8,[42] we did not observe significant apoptotic activity in TRAMP tumors. It is interesting that the active 35-kDa form of caspase-9 was observed only in the wild-type mice. However, there did not appear to be a significant amount of active caspase-3 detected in either wild-type or *Xiap*-deficient mice. This finding correlates with the relatively low apoptotic indices in these tumors as assessed by TUNEL staining. The absence of an effective apoptotic stimulus may have negated any effect from *Xiap* deficiency. Synergy between XIAP antagonism has been seen when combined with an apoptosis-inducing stimulus, even if little effect is seen in the absence of such a stimulus. Future combinations of chemotherapy or radiation therapy with XIAP antagonism in this or other transgenic cancer models may help resolve this possibility. XIAP antagonists may also have more clinical efficacy if combined with traditional cytotoxic therapies.

Given the promising preclinical reports of XIAP-targeted therapy, it is not surprising that these agents are being developed for clinical use. XIAP is a particularly attractive therapeutic target, because the apparent health of *Xiap*-deficient mice suggests that the side effects of suppressing XIAP should be minimal. The present study is, to our knowledge, the first evaluation of the role of XIAP in an immunocompetent autochthonous tumor model. Contrary to the previously discussed preclinical reports, we did not observe a protective effect in *Xiap*-deficient mice. Moreover, the suggestion of an adverse impact of *Xiap* deficiency on tumor progression, in addition to previous accounts of an adverse prognosis associated with low XIAP levels in prostate and lung cancer, underscores the need for a better understanding of the physiologic function of XIAP. These findings have obvious implications for treatments targeting XIAP activity. Neoplastic cells likely develop antiapoptotic mechanisms that do not depend on XIAP overexpression, which may have greater importance in the setting of XIAP antagonism. Greater insight into these pathways will help in selection of patients who would benefit most from XIAP-targeted therapies, as well as in overcoming resistance to such therapies.

Materials and Methods

Animals. Generation and genotyping of TRAMP and *Xiap*-deficient mice have been previously described.[27,30] All mice were bred and maintained on a C57BL/6 background. TRAMP males were mated with $Xiap^{+/-}$ females to generate $Xiap^{-}$ TRAMP males, as well as $Xiap^{+}$ TRAMP males for controls. Research was conducted on a UCUCA-approved protocol in a manner consistent with the NIH Guidelines for the Care and Use of Laboratory Animals. Beginning at 12 weeks of age, weekly abdominal palpation by two independent observers was used to determine tumor onset. Mice were euthanized when moribund and samples were taken for histology, RNA and protein evaluation. The pelvic lymph nodes and the abdominal and thoracic cavities were observed for signs of metastasis and visible metastases were confirmed histologically.

MRI imaging. Mice were imaged with abdominal MRI biweekly by the Michigan Small Animal Imaging Resource (http://www.med.umich.edu/msair). Mice were anesthetized with 2% isoflurane–air mixture. Images were obtained with a 7.0T Varian MR scanner (183-mm horizontal bore; Varian, Palo Alto, CA, USA). A double-tuned volume radiofrequency coil was used to scan the abdominal region of the mice. Axial T_2-weighted images were acquired using a fast spin-echo sequence with the following parameters: repetition time/effective echo time, 4000/60 ms; echo spacing, 15 ms; number of echoes, 8; field of view 30 mm $\times$ 30 mm; matrix, 128 $\times$ 128; slice thickness, 1 mm; slice spacing, 0.25 mm; number of slices, 17 and number of scans, 4 (total scan time was approximately 4 min.).

Immunoblot. Previously frozen specimens were lysed on ice in radioimmunoprecipitation analysis buffer containing protease inhibitors. Membranes were probed using a 1 : 2000 dilution of rodent inhibitor of apoptosis protein (RIAP) rabbit polyclonal antibody (a gift from Peter Liston and Robert Korneluk), which recognizes mouse c-IAP1 and c-IAP2. Immunoblots were also probed for XIAP (goat polyclonal, R&D, cat no. AF8221, Minneapolis, MN, USA), caspase-3 (rabbit polyclonal, a gift from Guy Salvesen) and caspase-9 (mouse monoclonal, Stressgen, cat no. AAM-139, Ann Arbor, MI, USA). β-Actin antibody was purchased from Sigma (St Louis, MO, USA). The following HRP-conjugated secondary antibodies were used: sheep anti-mouse (Amersham, Piscataway, NJ, USA), donkey anti-rabbit (Amersham) and donkey anti-goat (Serotec, Raleigh, NC, USA). Densitometry was performed by NIH ImageJ software (http://rsb.info.nih.gov/ij/).

Quantitative RT-PCR. Tissue specimens were preserved in RNAlater (Ambion, Austin, TX, USA). RNA was extracted using an RNeasy kit (Qiagen, Valencia, CA, USA). cDNA was generated using RTScript reverse transcriptase and quantified using TaqMan gene expression assays (Applied Biosystems, Foster City, CA, USA) on an ABI 7500 qPCR instrument.

Histology. Hematoxylin and eosin-stained slides were prepared from paraffin-embedded formalin-fixed tissue by the University of Michigan Tissue core. Slides were examined in a blinded fashion by a certified genitourinary pathologist (KJW) and classified as phylloides, PIN, or carcinoma. Carcinoma specimens were graded as well, moderately or poorly differentiated. Liver and lung sections were similarly inspected. TUNEL staining was performed with the Apoptag kit (Chemicon, Temecula, CA, USA) by the University of Michigan Tissue core. Digital images of five independent fields were taken of each tumor at $\times$ 40 magnification. TUNEL-positive cells were counted manually, while total cell number was determined by ImageJ analysis. Quantification was recorded as the number of TUNEL-positive cells per 1000 cells. Mitotic and proliferative indices were calculated in an analogous manner, although images were visualized at $\times$ 100 to facilitate the identification of mitotic figures. Ki-67 staining was also performed by the University of Michigan Tissue core using a primary antibody from Dako (Carpinteria, CA, USA) and the MOM immunodetection kit from Vector Laboratories (Burlingame, CA, USA).

Statistical analysis. Statistical analysis for Kaplan–Meier plots was performed using a two-sided log-rank test. In addition, a one-sided log-rank test was used to determine whether the knockout mice had better outcomes than the wild-type mice. All other comparisons were performed using a two-tailed χ^2 test. Calculations were performed using the R statistical computation system (http://www.R-project.org). Values of $P<0.05$ were considered statistically significant.

Acknowledgements. We thank Drs. Peter Liston and Robert Korneluk for the generous gift of RIAP antibody, Dr. Guy Salvesen for his gift of caspase-3 antibody and Drs. Brian Ross and Brad Moffat for their assistance with MRI imaging. KO is a recipient of a Pre-doctoral Award funded through the Breast Cancer Research Program of the Department of Defense (W81XWH-06-1-0429). This study was supported by funding received from the Department of Defense

(W81XWH-04-1-0891) and the National Institutes of Health (5R01GM067827-03). Dr. Colin Duckett serves as a consultant to Aegera Therapeutics and is a member of their scientific advisory board. All other authors have no conflicting interests.

1. Hanahan D, Weinberg RA. The hallmarks of cancer. *Cell* 2000; **100**: 57–70.
2. Green DR, Evan GI. A matter of life and death. *Cancer Cell* 2002; **1**: 19–30.
3. Nunez G, Benedict MA, Hu Y, Inohara N. Caspases: the proteases of the apoptotic pathway. *Oncogene* 1998; **17**: 3237–3245.
4. Shiozaki EN, Shi Y. Caspases, IAPs and Smac/DIABLO: mechanisms from structural biology. *Trends Biochem Sci* 2004; **29**: 486–494.
5. Vaux DL, Silke J. IAPs, RINGs and ubiquitylation. *Nat Rev Mol Cell Biol* 2005; **6**: 287–297.
6. Deveraux QL, Takahashi R, Salvesen GS, Reed JC. X-linked IAP is a direct inhibitor of cell-death proteases. *Nature* 1997; **388**: 300–304.
7. LaCasse EC, Baird S, Korneluk RG, MacKenzie AE. The inhibitors of apoptosis (IAPs) and their emerging role in cancer. *Oncogene* 1998; **17**: 3247–3259.
8. Holcik M, Gibson H, Korneluk RG. XIAP: apoptotic brake and promising therapeutic target. *Apoptosis* 2001; **6**: 253–261.
9. Schimmer AD, Dalili S, Batey RA, Riedl SJ. Targeting XIAP for the treatment of malignancy. *Cell Death Differ* 2006; **13**: 179–188.
10. Jaffer S, Orta L, Sunkara S, Sabo E, Burstein DE. Immunohistochemical detection of antiapoptotic protein X-linked inhibitor of apoptosis in mammary carcinoma. *Hum Pathol* 2007; **38**: 864–870.
11. Kluger HM, McCarthy MM, Alvero AB, Sznol M, Ariyan S, Camp RL *et al.* The X-linked inhibitor of apoptosis protein (XIAP) is up-regulated in metastatic melanoma, and XIAP cleavage by phenoxodiol is associated with carboplatin sensitization. *J Transl Med* 2007; **5**: 6.
12. Krajewska M, Krajewski S, Banares S, Huang X, Turner B, Bubendorf L *et al.* Elevated expression of inhibitor of apoptosis proteins in prostate cancer. *Clin Cancer Res* 2003; **9**: 4914–4925.
13. Lopes RB, Gangeswaran R, McNeish IA, Wang Y, Lemoine NR. Expression of the IAP protein family is dysregulated in pancreatic cancer cells and is important for resistance to chemotherapy. *Int J Cancer* 2007; **120**: 2344–2352.
14. Mizutani Y, Nakanishi H, Li YN, Matsubara H, Yamamoto K, Sato N *et al.* Overexpression of XIAP expression in renal cell carcinoma predicts a worse prognosis. *Int J Oncol* 2007; **30**: 919–925.
15. Tamm I, Richter S, Oltersdorf D, Creutzig U, Harbott J, Scholz F *et al.* High expression levels of X-linked inhibitor of apoptosis protein and survivin correlate with poor overall survival in childhood *de novo* acute myeloid leukemia. *Clin Cancer Res* 2004; **10**: 3737–3744.
16. Tamm I, Kornblau SM, Segall H, Krajewski S, Welsh K, Kitada S *et al.* Expression and prognostic significance of IAP-family genes in human cancers and myeloid leukemias. *Clin Cancer Res* 2000; **6**: 1796–1803.
17. Berezovskaya O, Schimmer AD, Glinskii AB, Pinilla C, Hoffman RM, Reed JC *et al.* Increased expression of apoptosis inhibitor protein XIAP contributes to anoikis resistance of circulating human prostate cancer metastasis precursor cells. *Cancer Res* 2005; **65**: 2378–2386.
18. Holcik M, Yeh C, Korneluk RG, Chow T. Translational upregulation of X-linked inhibitor of apoptosis (XIAP) increases resistance to radiation induced cell death. *Oncogene* 2000; **19**: 4174–4177.
19. Liu Z, Li H, Derouet M, Filmus J, LaCasse EC, Korneluk RG *et al. ras* oncogene triggers up-regulation of cIAP2 and XIAP in intestinal epithelial cells: epidermal growth factor receptor-dependent and -independent mechanisms of *ras*-induced transformation. *J Biol Chem* 2005; **280**: 37383–37392.
20. Liu Z, Li H, Wu X, Yoo BH, Yan SR, Stadnyk AW *et al.* Detachment-induced upregulation of XIAP and cIAP2 delays anoikis of intestinal epithelial cells. *Oncogene* 2006; **25**: 7680–7690.
21. Ng CP, Bonavida B. X-linked inhibitor of apoptosis (XIAP) blocks Apo2 ligand/tumor necrosis factor-related apoptosis-inducing ligand-mediated apoptosis of prostate cancer cells in the presence of mitochondrial activation: sensitization by overexpression of second mitochondria-derived activator of caspase/direct IAP-binding protein with low pI (Smac/DIABLO). *Mol Cancer Ther* 2002; **1**: 1051–1058.
22. Nomura T, Mimata H, Takeuchi Y, Yamamoto H, Miyamoto E, Nomura Y. The X-linked inhibitor of apoptosis protein inhibits taxol-induced apoptosis in LNCaP cells. *Urol Res* 2003; **31**: 37–44.
23. Amantana A, London CA, Iversen PL, Devi GR. X-linked inhibitor of apoptosis protein inhibition induces apoptosis and enhances chemotherapy sensitivity in human prostate cancer cells. *Mol Cancer Ther* 2004; **3**: 699–707.
24. LaCasse EC, Cherton-Horvat GG, Hewitt KE, Jerome LJ, Morris SJ, Kandimalla ER *et al.* Preclinical characterization of AEG35156/GEM 640, a second-generation antisense oligonucleotide targeting X-linked inhibitor of apoptosis. *Clin Cancer Res* 2006; **12**: 5231–5241.
25. McManus DC, Lefebvre CA, Cherton-Horvat G, St-Jean M, Kandimalla ER, Agrawal S *et al.* Loss of XIAP protein expression by RNAi and antisense approaches sensitizes cancer cells to functionally diverse chemotherapeutics. *Oncogene* 2004; **23**: 8105–8117.
26. Ferreira CG, van der Valk P, Span SW, Ludwig I, Smit EF, Kruyt FA *et al.* Expression of X-linked inhibitor of apoptosis as a novel prognostic marker in radically resected non-small cell lung cancer patients. *Clin Cancer Res* 2001; **7**: 2468–2474.
27. Greenberg NM, DeMayo F, Finegold MJ, Medina D, Tilley WD, Aspinall JO *et al.* Prostate cancer in a transgenic mouse. *Proc Natl Acad Sci USA* 1995; **92**: 3439–3443.
28. Bilim V, Kasahara T, Hara N, Takahashi K, Tomita Y. Role of XIAP in the malignant phenotype of transitional cell cancer (TCC) and therapeutic activity of XIAP antisense oligonucleotides against multidrug-resistant TCC *in vitro*. *Int J Cancer* 2003; **103**: 29–37.
29. Eckelman BP, Salvesen GS. The human anti-apoptotic proteins cIAP1 and cIAP2 bind but do not inhibit caspases. *J Biol Chem* 2006; **281**: 3254–3260.
30. Harlin H, Reffey SB, Duckett CS, Lindsten T, Thompson CB. Characterization of XIAP-deficient mice. *Mol Cell Biol* 2001; **21**: 3604–3608.
31. Yang Y, Fang S, Jensen JP, Weissman AM, Ashwell JD. Ubiquitin protein ligase activity of IAPs and their degradation in proteasomes in response to apoptotic stimuli. *Science* 2000; **288**: 874–877.
32. Marienfeld C, Yamagiwa Y, Ueno Y, Chiasson V, Brooks L, Meng F *et al.* Translational regulation of XIAP expression and cell survival during hypoxia in human cholangiocarcinoma. *Gastroenterology* 2004; **127**: 1787–1797.
33. Cummins JM, Kohli M, Rago C, Kinzler KW, Vogelstein B, Bunz F. X-linked inhibitor of apoptosis protein (XIAP) is a nonredundant modulator of tumor necrosis factor-related apoptosis-inducing ligand (TRAIL)-mediated apoptosis in human cancer cells. *Cancer Res* 2004; **64**: 3006–3008.
34. Ravi R, Fuchs EJ, Jain A, Pham V, Yoshimura K, Prouser T *et al.* Resistance of cancers to immunologic cytotoxicity and adoptive immunotherapy via X-linked inhibitor of apoptosis protein expression and coexisting defects in mitochondrial death signaling. *Cancer Res* 2006; **66**: 1730–1739.
35. Arnt CR, Chiorean MV, Heldebrant MP, Gores GJ, Kaufmann SH. Synthetic Smac/DIABLO peptides enhance the effects of chemotherapeutic agents by binding XIAP and cIAP1 *in situ*. *J Biol Chem* 2002; **277**: 44236–44243.
36. Sasaki H, Sheng Y, Kotsuji F, Tsang BK. Down-regulation of X-linked inhibitor of apoptosis protein induces apoptosis in chemoresistant human ovarian cancer cells. *Cancer Res* 2000; **60**: 5659–5666.
37. Schimmer AD, Welsh K, Pinilla C, Wang Z, Krajewska M, Bonneau MJ *et al.* Small-molecule antagonists of apoptosis suppressor XIAP exhibit broad antitumor activity. *Cancer Cell* 2004; **5**: 25–35.
38. Bruckheimer EM, Brisbay S, Johnson DJ, Gingrich JR, Greenberg N, McDonnell TJ. Bcl-2 accelerates multistep prostate carcinogenesis *in vivo*. *Oncogene* 2000; **19**: 5251–5258.
39. Gupta S, Hastak K, Ahmad N, Lewin JS, Mukhtar H. Inhibition of prostate carcinogenesis in TRAMP mice by oral infusion of green tea polyphenols. *Proc Natl Acad Sci USA* 2001; **98**: 10350–10355.
40. Gupta S, Adhami VM, Subbarayan M, MacLennan GT, Lewin JS, Hafeli UO *et al.* Suppression of prostate carcinogenesis by dietary supplementation of celecoxib in transgenic adenocarcinoma of the mouse prostate model. *Cancer Res* 2004; **64**: 3334–3343.
41. Tenev T, Zachariou A, Wilson R, Ditzel M, Meier P. IAPs are functionally non-equivalent and regulate effector caspases through distinct mechanisms. *Nat Cell Biol* 2005; **7**: 70–77.
42. Yang L, Cao Z, Yan H, Wood WC. Coexistence of high levels of apoptotic signaling and inhibitor of apoptosis proteins in human tumor cells: implication for cancer specific therapy. *Cancer Res* 2003; **63**: 6815–6824.

BJ www.biochemj.org

BJ Signal

Biochem. J. (2009) **417**, 765–771 (Printed in Great Britain) doi:10.1042/BJ20081677

Cytoprotective effects of IAPs revealed by a small molecule antagonist

Stefanie GALBÁN*, Clara HWANG†, Julie M. RUMBLE*, Karolyn A. OETJEN*, Casey W. WRIGHT*, Alain BOUDREAULT‡, Jon DURKIN‡, John W. GILLARD‡, James B. JAQUITH‡, Stephen J. MORRIS‡ and Colin S. DUCKETT*†[1,2]

*Department of Pathology, University of Michigan, 1301 Catherine, 5240 Medical Science I, Ann Arbor, MI 48109, U.S.A., †Department of Internal Medicine, University of Michigan, 1500 East Medical Center Drive, Ann Arbor, MI 48109, U.S.A., and ‡Aegera Therapeutics, 810 Chemin du Golf, Montreal, QC, Canada, H3E 1A8

Deregulated expression of members of the *IAP* (inhibitor of apoptosis) family has been identified in a wide variety of neoplastic cells, and synthetic IAP antagonists represent a promising novel class of chemotherapeutic agents. Early work focused on the ability of these compounds to block the caspase-inhibitory function of XIAP (X-linked IAP). However, recent studies have shown that IAP antagonists, although primarily designed to target XIAP, trigger ubiquitin-mediated degradation of two related proteins, c-IAP (cellular IAP) 1 and c-IAP2, and through this process potentiates the death of tumour cells via autocrine cellular-signalling pathways. In this context, the relative contribution of XIAP as a target of this class of compounds is unclear. In the present study, we examine the involvement of XIAP using a recently described synthetic IAP antagonist, AEG40730, and through comparison of a human *XIAP*-depleted tumour cell line with its isogenic wild-type control line. Treatment with nanomolar concentrations of AEG40730 resulted in the loss of both XIAP and c-IAP1 proteins, albeit with different kinetics. Although *XIAP*-deficient HCT116 cells retained some sensitivity to external apoptotic stimuli, the results suggest that IAP antagonists, such as AEG40730, exert their apoptosis-enhancing effects through XIAP in addition to the c-IAPs. These results indicate that IAP antagonists can target multiple IAPs to augment distinct pro-apoptotic signalling pathways, thereby revealing the potential for these compounds in cancer therapy and underscoring the promise of IAP-targeted therapies.

Key words: apoptosis, caspase, inhibitor of apoptosis (IAP), second mitochondrial-derived activator of caspase (Smac), tumour-necrosis-factor-related apoptosis-inducing ligand (TRAIL).

INTRODUCTION

Homoeostatic regulation of metazoan cell number is dependent on a tightly regulated balance between the proliferation and death of cells [1,2]. Deregulation of this balance is a hallmark of many disease states, and the activities of key components of both the proliferative and apoptotic (programmed cell death) machinery are altered in a wide variety of disorders, including neurodegenerative, autoimmune and neoplastic diseases [3–5], and factors that influence this balance are of great significance in treating a host of diseases.

One important group of factors that regulate apoptosis is the TNF (tumour necrosis factor) receptor superfamily which, following engagement with its cognate ligands, can elicit pro-survival and/or pro-apoptotic responses [6]. Several TNF receptor family members have attracted much attention as therapeutic targets for the treatment of cancers and immunological disorders. For example, cells from a range of malignancies, including cancers of the prostate, colon and of hepatic origin, appear to be highly sensitive to the pro-apoptotic ligand TRAIL (TNF-related apoptosis-inducing ligand) [7–9], and this has led to the development of TRAIL ligands and agonists as potential therapeutic tools for cancer treatment.

The central effectors of apoptosis are caspases, a family of intracellular cysteine proteases with a specificity for aspartate-containing residues [10,11]. Caspases function in a hierarchical manner; they are synthesized initially as inactive zymogens and, following activation, upstream or initiator caspases, such as caspases 8 and 9, can become activated by oligomerization through a process referred to as the induced proximity model [12], which subsequently leads to the cleavage and activation of effector caspases, such as caspases 3 and 7.

IAP (inhibitor of apoptosis) proteins are a group of intracellular proteins, several of which have been shown to inhibit caspases directly [13]. IAPs are characterized by the presence of one or more BIR (baculoviral IAP repeat) domains, which bind directly to caspases [14]. The most intensively studied IAP protein is XIAP (X-linked IAP), which contains three BIR domains. The most C-terminal BIR domain (BIR3) is necessary and sufficient for the binding and inhibition of caspase 9 by XIAP, whereas BIR2, together with a short proximal N-terminal domain, is involved in the binding and inhibition of caspases 3 and 7 [15,16]. Interestingly, XIAP expression has been shown to be elevated in several malignancies [17–19], and so has become a promising target in anticancer therapies.

The caspase-inhibitory property of XIAP can be neutralized by Smac (second mitochondrial-derived activator of caspase)/DIABLO (direct IAP-binding protein with low pI), a nuclear-encoded mitochondrial protein that is released into the cytosol following mitochondrial permeabilization [20,21]. Binding of Smac to XIAP can displace the XIAP–caspase interaction, releasing the caspase and lowering the cellular apoptotic threshold. Many seminal studies have revealed the nature of the Smac–XIAP interaction [20–23], and a number of synthetic compounds have been developed that resemble the XIAP-interacting interface in Smac. Interestingly, several of these compounds have also been found to interact with at least two other IAPs, c-IAP (cellular IAP) 1 and c-IAP2, even though the

Abbreviations used: BIR, baculoviral IAP repeat; GFP, green fluorescent protein; HEK-293 cell, human embryonic kidney cell; IAP, inhibitor of apoptosis; c-IAP, cellular IAP; DIABLO, direct IAP-binding protein with low pI; PI, propidium iodide; Smac, second mitochondrial-derived activator of caspase; TNF, tumour necrosis factor; TRAIL, TNF-related apoptosis-inducing ligand; XIAP, X-linked IAP.

[1] C.S.D. is a consultant for Aegera Therapeutics Inc.

[2] To whom correspondence should be addressed (email colind@umich.edu).

experimental strategies leading to their discovery were based on the XIAP–Smac/DIABLO interaction paradigm. These results suggest that targeting c-IAP1 and c-IAP2 with Smac mimetics results in a lowering of the apoptotic threshold indirectly, by affecting the activation of the NF-κB transcriptional network, rather than by relieving the constraints on caspases directly [24–26]. Much less clear, however, is the relative contribution of XIAP to the pro-apoptotic effects of these compounds, and how suitable XIAP may be as a future molecular target for drug design.

In the present study, we examine the role of XIAP in TRAIL-induced apoptosis by comparing apoptotic signalling in an XIAP-expressing cell line with a derivative line in which XIAP was ablated by homologous recombination. Using this approach, we compared the effects of combined treatment of TRAIL or TNF with AEG40730, an IAP inhibitor identified recently. We found that AEG40730 can induce the degradation of the c-IAPs, and this is likely to be of central importance when compounds such as AEG40730 are used to sensitize cells to the cytotoxic effects of TNF. Interestingly, in addition to targeting c-IAPs, AEG40730 also triggered the degradation of XIAP, and this combined effect was found to augment cell killing significantly when utilized in combination with TRAIL or TNF. These findings reveal that Smac antagonists, such as AEG40730, target multiple IAPs, including XIAP, to potentiate apoptosis, and underscores the therapeutic potential of these compounds in combination with different primary apoptotic inducers.

EXPERIMENTAL

Cell culture, infections and plasmids

Wild-type, *XIAP*-deficient and *BAX*-deficient HCT116 cells [27], kindly provided by Dr Bert Vogelstein (School of Medicine, Johns Hopkins University, Baltimore, MD, U.S.A.), were cultured in McCoy's 5A medium containing 10 % (v/v) FBS (fetal bovine serum) supplemented with 2 mM glutamax at 37 °C in an atmosphere of 5 % CO_2.

The lentiviral expression vector FG9 was constructed by modification of the shRNA (small hairpin RNA) vector FG12 [28] to include the EF-1a (elongation factor 1α) promoter and a multiple cloning site from the expression plasmid pEBB [29]. FG9/GFP-hygro (where GFP is green fluorescent protein and hygro is hygromycin B) was constructed by replacing the GFP cassette in FG9 with a GFP–hygromycin resistance fusion construct. Further details of the construction of these plasmids are available upon request.

The coding sequences of native XIAP, XIAP D148A, XIAP E219R/H223V, XIAP W310A, XIAP D148A/W310A, XIAP H467A and Bcl-x_L were subcloned from pEBB into the BamHI and NotI sites of FG9EF-1a. For stable cell line preparation, the FG9EF-1a empty vector (control) or XIAP and the XIAP mutants in the FG9EF-1a vector were co-transfected with pHCMV-G, pRRE and pRSVrev [28], which direct expression of lentiviral structural proteins, into HEK-293 cells (human embryonic kidney cells) using a standard calcium phosphate transfection protocol [29a] and incubated at 37 °C in an atmosphere of 7 % CO_2. The virus-containing medium on the HEK-293 cells was collected at 40 h post-transfection, polybrene (Sigma) was added to a final concentration of 25 mM and the medium was filtered through a 0.45-mm-pore size Millex HV PVDF filter unit (Millipore) on to HCT116 cells. The virus was incubated with the HCT116 cells for 4 h, followed by addition of fresh McCoy's medium and incubation for an additional 48 h at 37 °C in an atmosphere of 7 % CO_2. Stable cells were selected by the addition of 200 mg/ml hygromycin B (Invitrogen).

Viability experiments

HCT116 were seeded into six-well dishes (5×10^5–6×10^5 cells/well) and stimulated with the indicated doses of recombinant TRAIL (Alexis Biochemicals) for 2 h unless stated otherwise. For experiments with TNF (Roche Diagnostics), a dose of 200 units/ml was used for either 5 or 18 h. After treatment with TRAIL or TNF, cells were washed with PBS and recovered in fresh medium as indicated in the Figure legends (24 or 48 h). For experiments with the IAP antagonist AEG40730, cells were pre-treated for 24 h with a final concentration of 10 or 100 nM AEG40730 or DMSO as vehicle control. At the indicated time points, cells were collected by trypsinization, subsequent centrifugation and resuspension in PBS plus 1 % BSA and 2 μg/ml PI (propidium iodide). The cell viability of PI-stained cells was analysed by flow cytometry using a Coulter EPICS model XL-MCL flow cytometer (Beckman Coulter).

Protein extraction and immunoblotting

Whole cell lysates were prepared using RIPA buffer [1 % NP-40 (nonidet P40), 0.5 % sodium deoxycholate, 0.1 % SDS, 1 mM DTT (dithiothreitol) and 1 mM PMSF] supplemented with protease inhibitors. Samples were resolved by SDS/PAGE (4–12 % gradient gels) (Invitrogen), transferred on to nitrocellulose membranes (Invitrogen) and blocked in 5 % (w/v) non-fat dried skimmed milk powder in Tris-buffered saline containing 0.1 % Tween 20. Membranes were incubated at room temperature (20–25 °C) for 1 h with the following antibodies: XIAP (BD Pharmingen), β-actin (Sigma), Bcl-x_L (BD Pharmingen), BAX (Santa Cruz Biotechnology) or c-IAP1 [24]. Secondary horseradish-peroxidase-conjugated anti-mouse, anti-rabbit or anti-rat antibodies (GE Healthcare) were used for 1 h at room temperature. ECL® (enhanced chemiluminescence) (GE Healthcare) and Kodak XAR film were used for visualization purposes.

RESULTS

XIAP modulates the sensitivity to TRAIL-mediated apoptosis

Multiple IAP-targeting properties of Smac-like IAP antagonists have been described recently [24–26]. Less clear, however, are the relative contributions of specific IAPs to the apoptosis-promoting effects of these compounds, and whether these contributions differ depending on the type of apoptotic stimulus. To explore this question, we utilized the HCT116 human colon carcinoma cell line and a derivative line in which the *XIAP* gene had been disrupted by homologous recombination [27]. These cell lines were first examined for their responsiveness to two different apoptotic stimuli, TRAIL and TNF. *XIAP*-null cells were found to be highly susceptible to TRAIL-induced apoptosis after prolonged stimulation (Figure 1A), consistent with results reported previously [27]. Neither cell line appeared to be susceptible to treatment with TNF alone, but the *XIAP*-deficient cell line was found to be highly sensitive to TNF compared with the parental cell line when co-incubated with the protein synthesis inhibitor cycloheximide (Figure 1B). These observations defined a set of experimental conditions under which XIAP plays a clear anti-apoptotic role, and provided a framework in which the effects of IAP antagonists could be examined.

Potentiation of TRAIL-induced apoptosis by a synthetic IAP antagonist

The IAP antagonist AEG40730 is a cell-permeable synthetic molecule with nanomolar affinities not only for XIAP, but also for

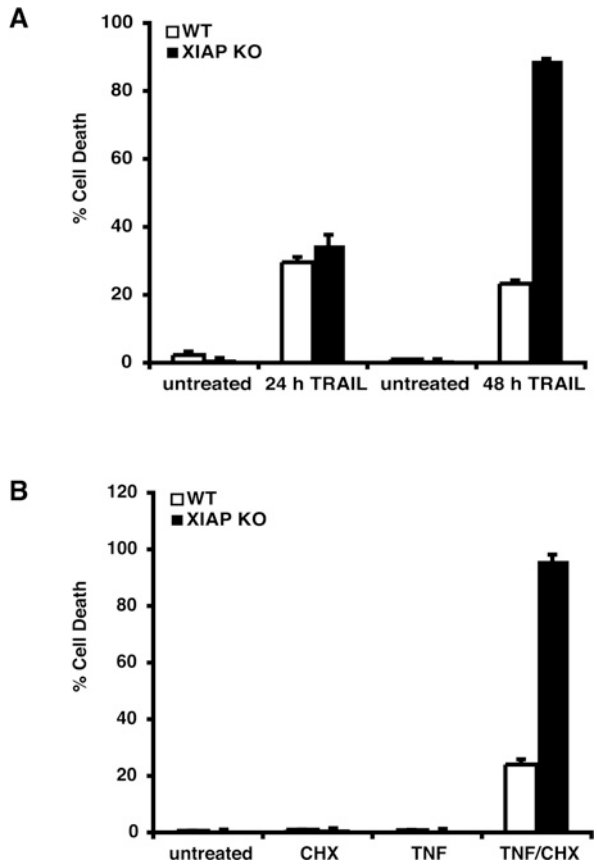

Figure 1 XIAP-dependent differences in sensitivity to TRAIL and TNF

(**A**) Parental (WT) and *XIAP*-deficient (XIAP KO) HCT116 cells were pulsed as indicated with TRAIL (75 ng/ml) for 2 h, and subsequently maintained in fresh medium for 24 or 48 h. Cell death was assessed by PI staining and subsequent flow cytometry. Results are means ± S.D. ($n \geqslant 3$). (**B**) Parental (WT) and *XIAP*-deficient (XIAP KO) HCT116 cells were treated with TNF (200 units/ml) for 18 h, cycloheximide (5 μg/ml) or TNF plus cycloheximide (TNF/CHX). Cells were then washed with PBS and maintained in fresh medium for 48 h, before staining with PI and analysis by flow cytometry. Results are means ± S.D. ($n = 3$) with each experiment performed in triplicate.

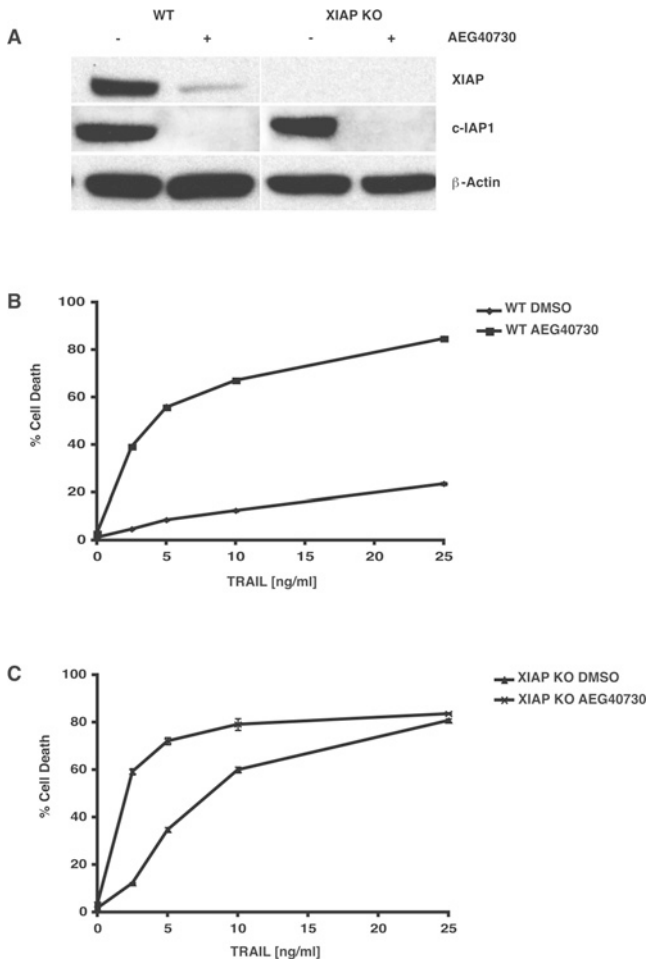

Figure 2 AEG40730 triggers the degradation of IAPs

(**A**) Parental (WT) and *XIAP*-deficient (XIAP KO) HCT116 cells were treated with AEG40730 (10 nM) for 24 h. Whole-cell lysates (15 μg) were resolved by SDS/PAGE and immunoblotted with XIAP, c-IAP1 or β-actin antibodies as indicated. A representative immunoblot is shown. (**B**) Parental HCT116 cells (WT) were treated with vehicle control (DMSO) or AEG40730 (10 nM) for 24 h, after which they were either left untreated or treated with a range of concentrations of TRAIL (2.5, 5, 10 and 25 ng/ml) for 2 h. Following 48 h recovery in fresh medium, PI-stained cells were analysed by flow cytometry. Results are means ± S.D. ($n = 3$) with each experiment performed in triplicate. (**C**) *XIAP*-deficient HCT116 cells (XIAP KO) were incubated with a vehicle control (DMSO) or with 10 nM AEG40730. After 24 h, recombinant TRAIL (2.5, 5, 10 and 25 ng/ml) was added to the treatment group for 2 h. Cells were then washed with PBS and the medium was replaced. Cell death was analysed by PI exclusion and flow cytometry after 48 h. Results are means ± S.D. ($n \geqslant 3$) with each experiment performed in triplicate.

c-IAP1 and c-IAP2 [30]. To examine its effects on IAP levels in the parental and *XIAP*-deficient HCT116 lines, cells were treated with AEG40730 and lysates prepared from these cells were examined by immunoblotting with antibodies against both XIAP and c-IAP1. In the parental line, XIAP protein levels were drastically diminished even at low concentrations of the drug (10 nM) after incubation for 24 h (Figure 2A), suggesting degradation of XIAP protein is induced by the drug. Importantly, c-IAP1 protein levels were also reduced under the same conditions (Figure 2A), and since this reduction occurred in both the parental and *XIAP*-deficient HCT116 cells, the targeting of c-IAP1 by AEG40730 appears to occur independently of XIAP.

In pilot studies, we found that HCT116 cells could tolerate a wide range of AEG40730 concentrations when delivered as a single agent, without considerable loss of viability (results not shown). To determine whether AEG40730 could potentiate apoptosis via a second signal in our defined system, HCT116 parental cells were pre-incubated with the drug, pulsed with TRAIL and subsequently examined for viability. The combination of TRAIL and AEG40730 induced a significant level of death, even at the lowest concentrations of TRAIL (Figure 2B), presumably as a consequence of the drug targeting one or more IAPs for degradation. The involvement of XIAP was therefore examined using identical experimental conditions, but titrating TRAIL into the *XIAP*-deficient HCT116 line. Interestingly, *XIAP*-null cells, while being more sensitive to TRAIL alone, were also sensitized further by AEG40730 at low concentrations of TRAIL (Figure 2C). However, this significant sensitization to TRAIL by AEG40730 in *XIAP*-deficient cells was no longer apparent when TRAIL concentrations were increased. Taken together, these results suggest that AEG40730 potentiates cell death, especially at lower concentrations of TRAIL, by degrading several IAPs.

XIAP reconstitution restores TRAIL resistance in *XIAP*-deficient cells

To establish definitively whether XIAP is required for resistance to TRAIL-induced apoptosis, we reconstituted *XIAP*-null HCT116 cells with wild-type XIAP. Cells with reconstituted XIAP were found to be protected against TRAIL-induced cell death when

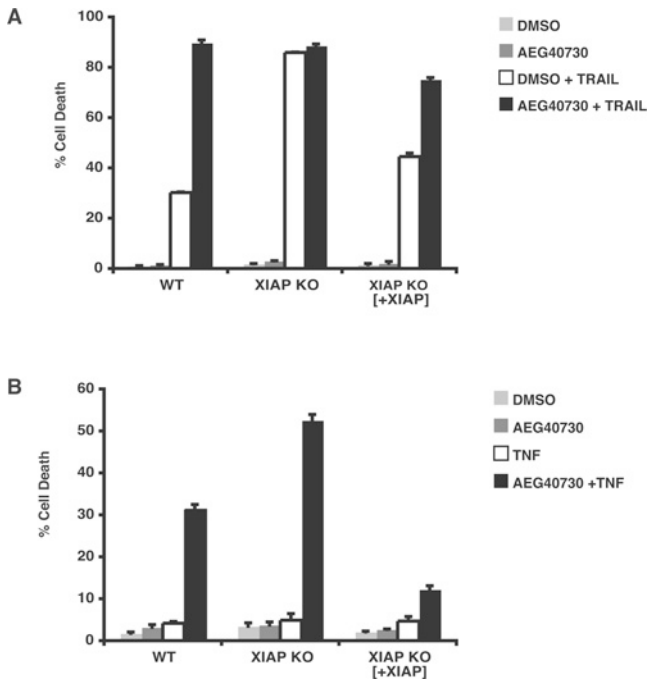

Figure 3 Reconstituted *XIAP*-null cells protect from TRAIL mediated death

(**A**) Parental (WT), *XIAP*-deficient (XIAP KO) and *XIAP*-deficient HCT116 cells reconstituted with XIAP (XIAP KO [+XIAP]) were pre-treated with DMSO or 10 nM AEG40730 for 24 h. Subsequently cells were either left untreated or treated for 2 h with 75 ng/ml TRAIL. Thereafter cells were washed with PBS and placed in fresh medium for 48 h. Cell death was measured by PI staining and flow cytometry. Results are means ± S.D. ($n \geqslant 3$) with each experiment performed in triplicate. (**B**) Parental (WT), *XIAP*-deficient (XIAP KO) and *XIAP*-deficient cells reconstituted with XIAP (XIAP KO [+XIAP]) were pre-treated with vehicle control (DMSO) or AEG40730 (10 nM) for 24 h. Cells were then left untreated or treated with TNF (200 units/ml) for 5 h, washed in PBS and recovered in fresh medium for 48 h. Apoptosis was measured by staining cells with PI and flow cytometry. Results are means ± S.D. ($n \geqslant 3$) with each experiment performed in triplicate.

compared with *XIAP*-deficient cells (Figure 3A), and cell death was potentiated when such cells were co-treated with AEG40730, to a similar degree to that observed in AEG40730-treated parental cells. These findings are strongly indicative of a role for XIAP in the resistance to TRAIL-induced death, which can be neutralized by exposure to this IAP antagonist.

Recent reports have demonstrated an important role of c-IAP1 and c-IAP2 in inhibiting TNF-mediated cell death [24–26]. We utilized the parental and *XIAP*-null HCT116 cells to evaluate the death response to TNF in the presence of AEG40730. Cells were pre-treated with AEG40730 and subsequently pulsed with TNF without cycloheximide. Parental HCT116 cells were not responsive to TNF (Figure 1B); however, when treated with AEG40730, the parental line became sensitized to TNF-induced apoptosis (Figure 3B). Interestingly, *XIAP*-deficient HCT116 cells did not die following incubation with TNF alone (Figure 1B), but were also further sensitized to TNF-induced killing by pre-treatment with AEG40730 (Figure 3B), similar to the effects observed with combined treatment of cells with AEG40730 and TRAIL. In both cases, overexpression of XIAP appeared to confer a significant degree of protection against cell death by these ligands. Taken together, our results suggest that, under these conditions, TNF-induced death is potentiated by degradation of c-IAPs and XIAP following treatment with AEG40730. Although XIAP was found to contribute to this potentiation, XIAP deficiency alone was not sufficient to result in cell death by TNF (Figures 1B and 3B).

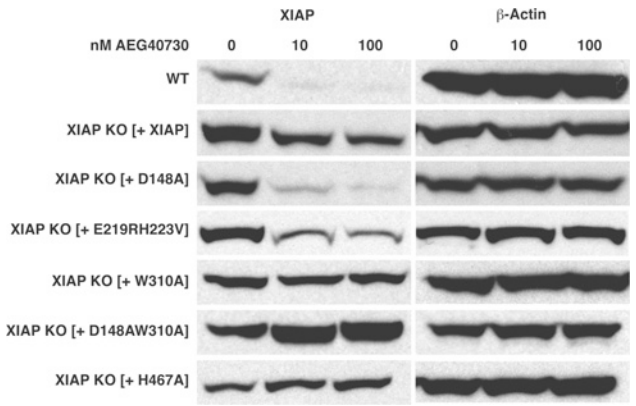

Figure 4 AEG40730 induces RING (really interesting new gene)-dependent degradation upon BIR3 binding

HCT116 wild-type (WT) and *XIAP*-null cells (XIAP KO) reconstituted with wild-type XIAP ([+XIAP]) or the indicated XIAP derivatives (XIAP D148A [+D148A], XIAP E219R/H223V [+E219RH223V], XIAP W310A [+W310A], XIAP D148A/W310A [+D148AW310A] and XIAP H467A [+H467A]) were treated with vehicle control (DMSO) or with 10 or 100 nM AEG40730 for 24 h. Whole-cell lysates from all cell lines were resolved by SDS/PAGE and immunoblotted with an antibody against XIAP or β-actin, as indicated. A representative Western blot of at least three independent experiments is shown.

Domains within XIAP are required for down-regulation by AEG40730

Most synthetic IAP antagonists are modelled on the N-terminal tetrapeptide of the IAP-binding motif in Smac/DIABLO, which binds to the BIR3 domains of all of the IAPs, and several of these have been shown recently to trigger the degradation of c-IAP1 and c-IAP2 [24–26]. To further explore the mechanism of XIAP inhibition by AEG40730, we reconstituted *XIAP*-deficient cells with wild-type XIAP or with XIAP derivatives bearing point mutations in the domains shown previously to be necessary for caspase inhibition and Smac binding. Cells were pre-incubated with AEG40730 at a range of concentrations and evaluated for changes in XIAP protein levels by immunoblotting. XIAP was degraded as a consequence of AEG40730 treatment in both the parental cells and the *XIAP*-deficient cell line in which XIAP had been reconstituted (Figure 4), although the reduction appeared to be less pronounced in the latter, probably as a result of the relatively high expression of the XIAP protein in these cells. As shown in Figure 4, AEG40730 treatment exerted a similar effect in cells reconstituted with an XIAP mutant encoding a protein incapable of inhibiting caspases 3 and 7 (XIAP D148A or XIAP E219R/H223V), but, interestingly, was unable to induce the degradation of a mutant version of XIAP (W310A) that is incapable of binding caspase 9, which presumably interferes with the binding site in BIR3 to which AEG40730 also binds. Under the same conditions (Figure 4), drug treatment of cells reconstituted with a doubly deficient XIAP derivative (XIAP D148A/W310A) also did not trigger degradation. Interestingly, AEG40730 was unable to induce degradation of XIAP in cells reconstituted with a mutant version of XIAP lacking its E3 ubiquitin-ligase activity (XIAP H467A). Taken together, these results suggest that XIAP is degraded by AEG40730 upon binding to BIR3 and that this degradation is probably mediated by a process involving autoubiquitination.

AEG40730 overcomes TRAIL resistance in cells overexpressing Bcl-x_L or lacking BAX

The pathological elevation of the *BCL2* gene family in many cancers has been shown to cause a loss in chemosensitivity [31],

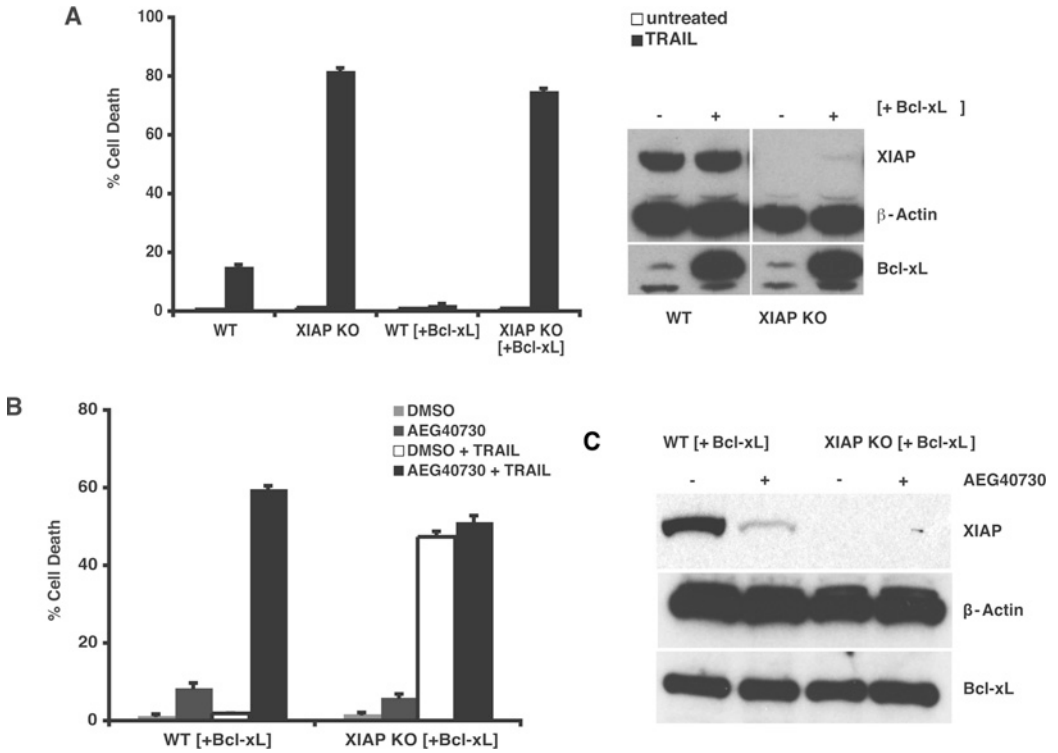

Figure 5 AEG40730 sensitizes Bcl-x_L-overexpressing parental cells to TRAIL

(**A**) Effects of TRAIL stimulation on cells stably overexpressing Bcl-x_L. HCT116 wild-type cells (WT), XIAP-null HCT116 cells (XIAP KO), HCT116 wild-type cells overexpressing Bcl-x_L (WT[+ Bcl-xL] and *XIAP*-null HCT116 cells overexpressing Bcl-x_L (XIAP KO[+ Bcl-xL] were stimulated with TRAIL as described in Figure 3, and viability was evaluated by PI exclusion. Right-hand panel: Whole-cell lysates were evaluated by immunoblotting with XIAP, Bcl-x_L and β-actin antibodies as indicated. (**B**) A combined treatment of AEG40730 and TRAIL on stably overexpressing Bcl-x_L wild-type HCT116 cells (WT[+ Bcl-xL]) and *XIAP*-null HCT116 cells (XIAP KO [+ Bcl-xL]) was performed by pre-incubating the cells for 24 h with AEG40730 (10 nM), followed by a 2 h stimulation of TRAIL (75 ng/ml). After a 24 h recovery period, cell death was assessed as described in Figure 3(A) legend. (**C**) Stably overexpressing Bcl-x_L wild-type HCT116 cells (WT[+ Bcl-xL]) and *XIAP*-null HCT116 cells (XIAP KO [+ Bcl-xL]) were either left untreated (−) or incubated with 10 nM AEG40730 (+). Whole-cell lysates (50 μg) were resolved by SDS/PAGE and immunoblotted using antibodies to XIAP, Bcl-x_L and β-actin, as indicated.

predominantly through interference with BH3 (Bcl-2 homology domain 3)-mediated activation of mitochondrial death pathways involving caspase 9. To examine whether AEG40730 can restore sensitivity to TRAIL under conditions of elevated Bcl-x_L, we introduced Bcl-x_L by lentiviral infection into parental and *XIAP*-deficient cells, and examined the sensitivity to TRAIL. Consistent with previous reports, parental cells overexpressing Bcl-x_L were greatly protected against TRAIL-induced death. However, when Bcl-x_L was stably expressed in *XIAP*-deficient cells, TRAIL was fully active in inducing cell death, and the resultant cell death was similar to that observed in *XIAP*-deficient cells without Bcl-x_L overexpression (Figure 5A). To examine whether AEG40730 could also reverse the observed resistance to TRAIL of Bcl-x_L-overexpressing cells, we co-treated such cells with AEG40730 and TRAIL. Combined treatment of AEG40730 and TRAIL fully restored sensitivity to TRAIL in Bcl-x_L-overexpressing cells, as depicted in Figure 5(B). Notably, pre-treatment with AEG40730 did not further sensitize *XIAP*-deficient cells overexpressing Bcl-x_L to TRAIL. As shown in Figure 5(C), Western blotting of XIAP confirmed that AEG40730 also reduced XIAP protein levels in cells with heightened Bcl-x_L expression. These results point to roles not only for the c-IAPs, but also for XIAP, in blocking TRAIL-induced apoptosis, in wild-type and in Bcl-x_L-overexpressing cells.

Ectopic expression of mature Smac/DIABLO and treatment with Smac antagonists have been shown to restore TRAIL sensitivity in cells that are deficient for the *BAX* gene [32]. To explore whether AEG40730 might be a useful means of restoring TRAIL responsiveness in this common resistance phenotype, HCT116 cells deficient for BAX were tested for sensitivity to AEG40730, either alone or in combination with TRAIL. AEG40730 alone did not induce cell death in *BAX*-deficient cells (Figure 6B), and *BAX*-deficient cells were fully resistant to TRAIL-induced death (Figure 6A). However, treatment of *BAX*-deficient cells with AEG40730 resulted in the reversal of resistance to TRAIL (Figure 6B), probably by attenuating IAP protein levels in these cells (Figure 6C). Although AEG40730 alone caused a reduction in XIAP protein levels, it did not induce cell death in *BAX*-deficient cells (Figure 6B). Taken together, these results suggest that AEG40730 can override the cytoprotective effects of elevated expression levels of Bcl-x_L, or conversely the reduced levels of *BAX*.

DISCUSSION

Acquired resistance to apoptotic stimuli is a hallmark of many neoplastic cells [33], and a major goal of chemotherapeutic strategies is to target and reactivate this pathway. Gaining a better understanding of how cancer cells evade apoptosis and become resistant to chemotherapy is essential for drug design and the development of novel treatment approaches. XIAP has been found

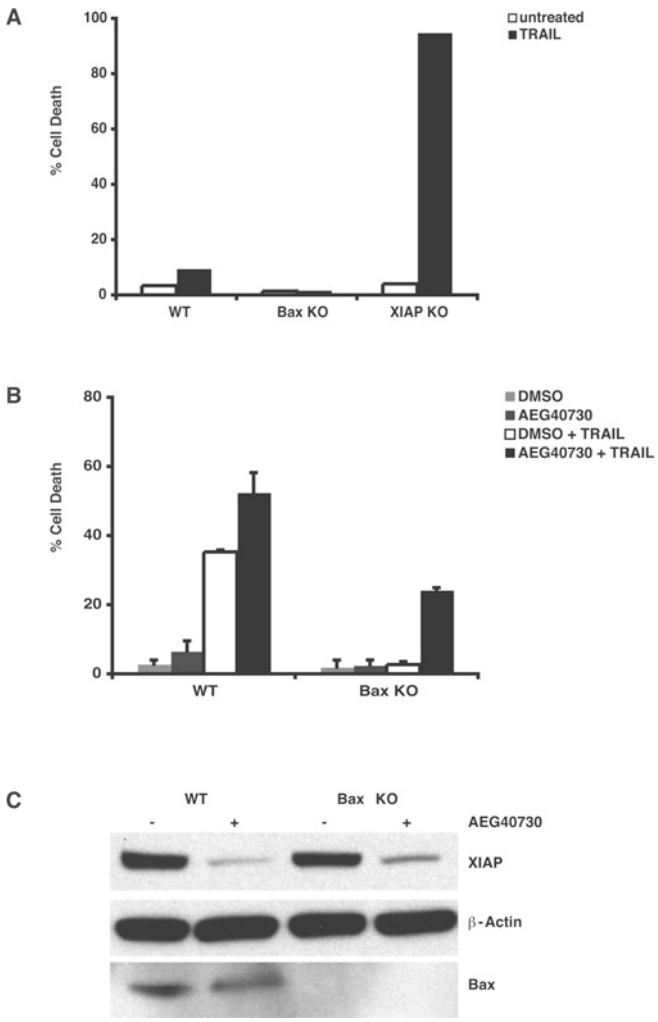

Figure 6 AEG40730 sensitizes *BAX*-deficient HCT116 cells to TRAIL

(**A**) Parental (WT), *BAX*-deficient (Bax KO) and *XIAP*-null (XIAP KO) cells were stimulated for 2 h with TRAIL (75 ng/ml). Cells were maintained in fresh medium for a further 48 h, and viability was examined as described in Figure 3(A) legend. Results are means ± S.D. ($n \geqslant 3$) with each experiment performed in triplicate. (**B**) Parental (WT) and *BAX*-deficient (Bax KO) HCT116 cells were pre-incubated for 24 h with AEG40730 (10 nM) and subsequently stimulated with TRAIL (75 ng/ml) for 2 h. (**C**) Parental (WT) and *BAX*-deficient (Bax KO) HCT116 cells were left untreated (−) or treated with 10 nM AEG40730 (+) for 24 h. Whole-cell lysates (15 μg) were resolved by SDS/PAGE and immunoblotted with XIAP, BAX and β-actin antibodies, as indicated.

to be overexpressed in many cancers, including colon cancer [17–19]. Antagonists or inhibitors of IAP-related proteins may serve as new tools, or indeed as exploratory therapeutics [34], and several XIAP antagonists and Smac mimetics [34,35] have been described previously and are advancing into clinical development. One remarkable effect of this class of molecules is their dramatic sensitization of cancer cells to death receptor ligands, such as TNF. The IAP antagonist AEG40730 differs in several structural aspects from the cases published previously, as it binds with low nanomolar affinity to the BIR3 domains of c-IAP1 and 2, as well as to XIAP. Treatment of cells with AEG40730 also triggers the profound degradation of c-IAP proteins (Figure 2 and results not shown), as well as of XIAP.

In the present study, we investigated the pro-apoptotic effects of the IAP antagonist AEG40730 in HCT116 cells when cells were co-treated with TRAIL. The results presented here indicate that AEG40730 greatly potentiates TRAIL-mediated apoptosis in this system (Figures 2B and 3A). Incubation with AEG40730 results in a marked reduction in c-IAP1 protein levels (Figure 2A), but since c-IAP1 levels were equally decreased in XIAP knockout cells, we interpret these results to indicate that potentiation of TRAIL-mediated cell death by AEG40730 is also dependent on its ability to neutralize XIAP. Recent reports have demonstrated the ability of IAP antagonists to induce apoptosis in a subset of sensitive cancer cells without the need of co-stimulators, such as TRAIL, TNF or other chemotherapeutic agents [24–26]. It was shown that this occurs through a TNF-mediated autocrine-secretion mechanism, acting upon TNF receptors, which requires the initial degradation of c-IAP1 and c-IAP2 by IAP-inhibiting molecules to induce apoptotic cell death mediated by caspase 8. In the present study, we compared the contribution of this process between TNF- and TRAIL-mediated killing, with a particular focus on the role played by XIAP. Our results suggest that the pro-apoptotic effect of AEG40730 in TRAIL-mediated cell death was dependent on the targeting not only of the c-IAPs, but also of XIAP. HCT116 cells were not responsive to TNF alone, but pre-treatment with AEG40730 resulted in dramatic sensitization to TNF-mediated death (Figure 3B). *XIAP*-deficient cells were also further sensitized to TNF by AEG40730, indicating that the sensitization by the drug to this stimulus is likely to be dependent on the elimination of other IAPs, such as the c-IAPs. The overexpression of XIAP in *XIAP*-null cells treated with AEG40730 partially rescued cells from TNF-mediated death (Figure 3B), consistent with its role as a potent inhibitor of caspase 3.

The observed involvement of XIAP in the pro-apoptotic function of AEG40730 in TRAIL-mediated death was further underscored by our finding that HCT116 wild-type cells with defects in the mitochondrial apoptotic pathway (*BAX*-null or Bcl-x_L overexpression) were sensitized to TRAIL when co-treated with AEG40730 (Figures 5B and 6B). Cell death in these cells was comparable with that observed in *XIAP*-deficient HCT116 cells or the same cells in which Bcl-x_L was ectopically expressed, treated with TRAIL alone or in combination with AEG40730 (Figures 5A and 5B). This confirms that XIAP contributed to TRAIL resistance in cells with an impairment in activation of the intrinsic mitochondrial apoptotic pathway. Taken together, these results suggest that AEG40730 can override the cytoprotective effects of heightened levels of Bcl-2 and Bcl-x_L, or conversely, reduced levels of pro-apoptotic members of the Bcl-2 family, such as BAX, that are found in many neoplastic diseases. Since the neutralization of XIAP to circumvent intrinsic mitochondrial death-signalling defects has been shown to restore TRAIL sensitivity and to bypass the ability of the tumour cell to evade immunotherapy and immune surveillance [31], the combination of cancer-selective drugs, such as TRAIL and IAP antagonists, represents a promising approach for cancer therapy.

ACKNOWLEDGEMENTS

We thank Dr D. Baltimore (Division of Biology, California Institute of Technology, Pasadena, CA, U.S.A.) for the FG12 expression plasmid, Dr B. Vogelstein (School of Medicine, Johns Hopkins University, Baltimore, MD, U.S.A) for cell lines, Dr J. Silke (Department of Biochemistry, LaTrobe University, VIC, Australia) for providing the antibody against c-IAP1, and members of the Duckett Laboratory for helpful discussions and critical reading of the manuscript.

FUNDING

This work was supported by the National Institutes of Health [grant number R01GM067827] and the Sandler Foundation to C. S. D. K. A. O. is a recipient of a pre-doctoral award

funded through the Breast Cancer Research Program of the Department of Defense [grant number W81XWH-06-1-0429] and S.G. is a recipient of a post-doctoral award (Lung Immunopathology Training Grant) from the National Institutes of Health [grant number NIH T32 HL07517].

REFERENCES

1 Letai, A. G. (2008) Diagnosing and exploiting cancer's addiction to blocks in apoptosis. Nat. Rev. Cancer **8**, 121–132
2 Rathmell, J. C. and Thompson, C. B. (2002) Pathways of apoptosis in lymphocyte development, homeostasis, and disease. Cell **109**, S97–S107
3 Kerr, J. F., Wyllie, A. H. and Currie, A. R. (1972) Apoptosis: a basic biological phenomenon with wide-ranging implications in tissue kinetics. Br. J. Cancer **26**, 239–257
4 Vaux, D. L., Haecker, G. and Strasser, A. (1994) An evolutionary perspective on apoptosis. Cell **76**, 777–779
5 Nagata, S. (1996) Apoptosis: telling cells their time is up. Curr. Biol. **6**, 1241–1243
6 Baud, V. and Karin, M. (2001) Signal transduction by tumor necrosis factor and its relatives. Trends Cell Biol. **11**, 372–377
7 Bucur, O., Ray, S., Bucur, M. C. and Almasan, A. (2006) APO2 ligand/tumor necrosis factor-related apoptosis-inducing ligand in prostate cancer therapy. Front. Biosci. **11**, 1549–1568
8 Hall, M. A. and Cleveland, J. L. (2007) Clearing the TRAIL for cancer therapy. Cancer Cell **12**, 4–6
9 Herr, I., Schemmer, P. and Buchler, M. W. (2007) On the TRAIL to therapeutic intervention in liver disease. Hepatology **46**, 266–274
10 Thornberry, N. A. and Lazebnik, Y. (1998) Caspases: enemies within. Science **281**, 1312–1316
11 Cryns, V. and Yuan, J. (1998) Proteases to die for. Genes Dev. **12**, 1551–1570
12 Muzio, M., Stockwell, B. R., Stennicke, H. R., Salvesen, G. S. and Dixit, V. M. (1998) An induced proximity model for caspase-8 activation. J. Biol. Chem. **273**, 2926–2930
13 Srinivasula, S. M. and Ashwell, J. D. (2008) IAPs: what's in a name? Mol. Cell **30**, 123–135
14 Vaux, D. L. and Silke, J. (2005) IAPs, RINGs and ubiquitylation. Nat. Rev. Mol. Cell Biol. **6**, 287–297
15 Deveraux, Q. L., Stennicke, H. R., Salvesen, G. S. and Reed, J. C. (1999) Endogenous inhibitors of caspases. J. Clin. Immunol. **19**, 388–398
16 Takahashi, R., Deveraux, Q., Tamm, I., Welsh, K., Assa-Munt, N., Salvesen, G. S. and Reed, J. C. (1998) A single BIR domain of XIAP sufficient for inhibiting caspases. J. Biol. Chem. **273**, 7787–7790
17 Tamm, I., Kornblau, S. M., Segall, H., Krajewski, S., Welsh, K., Kitada, S., Scudiero, D. A., Tudor, G., Qui, Y. H., Monks, A. et al. (2000) Expression and prognostic significance of IAP-family genes in human cancers and myeloid leukemias. Clin. Cancer Res. **6**, 1796–1803
18 Parton, M., Krajewski, S., Smith, I., Krajewska, M., Archer, C., Naito, M., Ahern, R., Reed, J. and Dowsett, M. (2002) Coordinate expression of apoptosis-associated proteins in human breast cancer before and during chemotherapy. Clin. Cancer Res. **8**, 2100–2108
19 Yang, L., Cao, Z., Yan, H. and Wood, W. C. (2003) Coexistence of high levels of apoptotic signaling and inhibitor of apoptosis proteins in human tumor cells: implication for cancer specific therapy. Cancer Res. **63**, 6815–6824
20 Du, C., Fang, M., Li, Y., Li, L. and Wang, X. (2000) Smac, a mitochondrial protein that promotes cytochrome *c*-dependent caspase activation by eliminating IAP inhibition. Cell **102**, 33–42
21 Verhagen, A. M., Ekert, P. G., Pakusch, M., Silke, J., Connolly, L. M., Reid, G. E., Moritz, R. L., Simpson, R. J. and Vaux, D. L. (2000) Identification of DIABLO, a mammalian protein that promotes apoptosis by binding to and antagonizing IAP proteins. Cell **102**, 43–53
22 Chai, J., Du, C., Wu, J. W., Kyin, S., Wang, X. and Shi, Y. (2000) Structural and biochemical basis of apoptotic activation by Smac/DIABLO. Nature **406**, 855–862
23 Srinivasula, S. M., Datta, P., Fan, X. J., Fernandes-Alnemri, T., Huang, Z. and Alnemri, E. S. (2000) Molecular determinants of the caspase-promoting activity of Smac/DIABLO and its role in the death receptor pathway. J. Biol. Chem. **275**, 36152–36157
24 Vince, J. E., Wong, W. W., Khan, N., Feltham, R., Chau, D., Ahmed, A. U., Benetatos, C. A., Chunduru, S. K., Condon, S. M., McKinlay, M. et al. (2007) IAP antagonists target cIAP1 to induce TNFα-dependent apoptosis. Cell **131**, 682–693
25 Varfolomeev, E., Blankenship, J. W., Wayson, S. M., Fedorova, A. V., Kayagaki, N., Garg, P., Zobel, K., Dynek, J. N., Elliott, L. O., Wallweber, H. J. et al. (2007) IAP antagonists induce autoubiquitination of c-IAPs, NF-κB activation, and TNFα-dependent apoptosis. Cell **131**, 669–681
26 Petersen, S. L., Wang, L., Yalcin-Chin, A., Li, L., Peyton, M., Minna, J., Harran, P. and Wang, X. (2007) Autocrine TNFα signaling renders human cancer cells susceptible to Smac-mimetic-induced apoptosis. Cancer Cell **12**, 445–456
27 Cummins, J. M., Kohli, M., Rago, C., Kinzler, K. W., Vogelstein, B. and Bunz, F. (2004) X-linked inhibitor of apoptosis protein (XIAP) is a nonredundant modulator of tumor necrosis factor-related apoptosis-inducing ligand (TRAIL)-mediated apoptosis in human cancer cells. Cancer Res. **64**, 3006–3008
28 Qin, X. F., An, D. S., Chen, I. S. and Baltimore, D. (2003) Inhibiting HIV-1 infection in human T cells by lentiviral-mediated delivery of small interfering RNA against CCR5. Proc. Natl. Acad. Sci. U.S.A. **100**, 183–188
29 Cheng, G. and Baltimore, D. (1996) TANK, a co-inducer with TRAF2 of TNF- and CD40L-mediated NF-κB activation. Genes Dev. **10**, 963–973
29a Duckett, C. S., Gedrich, R. W., Gilfillan, M. C. and Thompson, C. B. (1997) Induction of nuclear factor κB by the CD30 receptor is mediated by TRAF1 and TRAF2. Mol. Cell. Biol. **17**, 1535–1542
30 Bertrand, M. J., Milutinovic, S., Dickson, K. M., Ho, W. C., Boudreault, A., Durkin, J., Gillard, J. W., Jaquith, J. B., Morris, S. J. and Barker, P. A. (2008) cIAP1 and cIAP2 facilitate cancer cell survival by functioning as E3 ligases that promote RIP1 ubiquitination. Mol. Cell **30**, 689–700
31 Ravi, R., Fuchs, E. J., Jain, A., Pham, V., Yoshimura, K., Prouser, T., Jalla, S., Zhou, X., Garrett-Mayer, E., Kaufmann, S. H. et al. (2006) Resistance of cancers to immunologic cytotoxicity and adoptive immunotherapy via X-linked inhibitor of apoptosis protein expression and coexisting defects in mitochondrial death signaling. Cancer Res. **66**, 1730–1739
32 Kandasamy, K., Srinivasula, S. M., Alnemri, E. S., Thompson, C. B., Korsmeyer, S. J., Bryant, J. L. and Srivastava, R. K. (2003) Involvement of proapoptotic molecules Bax and Bak in tumor necrosis factor-related apoptosis-inducing ligand (TRAIL)-induced mitochondrial disruption and apoptosis: differential regulation of cytochrome c and Smac/DIABLO release. Cancer Res. **63**, 1712–1721
33 Hanahan, D. and Weinberg, R. A. (2000) The hallmarks of cancer. Cell **100**, 57–70
34 Vucic, D. and Fairbrother, W. J. (2007) The inhibitor of apoptosis proteins as therapeutic targets in cancer. Clin. Cancer Res. **13**, 5995–6000
35 Fischer, U. and Schulze-Osthoff, K. (2005) Apoptosis-based therapies and drug targets. Cell Death Differ. **12** (Suppl 1), 942–961

Received 15 August 2008/2 October 2008; accepted 14 October 2008
Published as BJ Immediate Publication 14 October 2008, doi:10.1042/BJ20081677